Investigation of Dioxin formation and destruction mechanisms in waste incineration plants in order to improve the quality of residues

Johanna Aurell and Stellan Marklund

Department of Chemistry
Umeå University

2008

Abstract

The study presented here was intended to identify combustion conditions that substantially reduce the formation of dioxins during MSW incineration, in order to decrease dioxin levels in the flue gas and thus in the flue gas cleaning residues. The study focused on PCDD/F formation, but PCBs and HCB were also considered. Sampling was performed in the post-combustion zone of a laboratory-scale fluidized-bed reactor. The parameters found to exert the greatest effect on dioxin formation were: sulphur and chlorine contents of the fuel, freeboard temperature and transient combustion conditions (incomplete combustion). An increase in the SO_2:HCl ratio from 0 to 0.4 reduced dioxin formation by 70%, but further increases in sulphur contents did not reduce dioxin production further.

An increase in chlorine level in the fuel from 0.7% to 1.7% resulted in a ten-fold increase in the dioxin levels, and a decrease in freeboard temperature from 800 °C to 660 °C resulted in about a three-fold increase in dioxin levels. Transient combustion conditions with increases in CO concentration from < 3 ppm (O_2=11%) to 1600 ppm (O_2=9%) resulted in the dioxin level increasing about 150-fold. A decrease in O_2 level from 10.9% to 2.4% with a simultaneous increase in the CO concentration from < 3 ppm to 1250 ppm resulted in dioxin levels increasing about seven-fold.

Dioxin formation was not observed under high-temperature (640 °C) conditions. The greatest dioxin formation rate was indicated to occur between 400 and 300 °C, with the amount and size of particulates being important determinants. The results also implied that a shorter residence time in this temperature range led to reductions in dioxin levels.

Concentrations of HCB and planar PCBs (dioxin-like PCBs) correlated with the I-TEQ levels observed for dioxins, while the sum of DIN-PCBs seemed to be unaffected, except by incomplete combustion.

Summary

Dioxins (PCDD/Fs) are known to form in the post-combustion zone during combustion of MSW incinerator. Dioxins are chlorinated aromatic compounds with high chemical stability and are persistent in the environment. Directive 2000/76 EC and Council Regulation (EC) 1195/2006 regulate the levels of PCDD/Fs in flue gases and the waste/residues, stipulating that they should not exceed 0.1 ng I-TEQ/Nm^3 and 15 µg I-TEQ/kg, respectively. The aim of the study presented here was to identify parameters that substantially affect the formation of PCDD/Fs during MSW incineration, in order to reduce dioxin formation in the flue gas and thus dioxin levels in the flue gas cleaning residues. The persistent organic pollutants (POPs) investigated were polychlorinated dibenzo-*p*-dioxins (PCDDs) and dibenzofurans (PCDFs), polychlorinated biphenyls (PCBs) and hexachlorobenzene (HCB), which are prioritized substances in the Stockholm POPs Convention. The primary focus of this study was on PCDD/F formation. The parameters with greatest effect on the formation of dioxins can be divided into two groups: fuel composition and combustion conditions. The parameters varied during this study were: temperature (in both the secondary-combustion zone and post-combustion zone); residence time in the post-combustion zone; fuel load; chlorine, copper, water and sulphur contents of the fuel; oxygen level in the flue gas and transient combustion conditions (incomplete combustion/increases in CO concentration). Twenty-three experimental runs were performed using Umeå University's laboratory-scale, fluidized-bed reactor (5 kW), which was constructed to simulate the behaviour of a full-scale waste incinerator, particularly with regard to the composition of the raw flue gas. The convector section allowed flue gas to be sampled at different points, with different temperatures and residence times. Both the secondary-combustion zone (freeboard) and the post-combustion zone (convector) temperatures were easily varied, with associated reductions or increases in flue gas residence time. The fuel used was an artificial municipal solid waste (MSW). This was homogenous and the composition was well known. On-line monitoring of O_2, H_2O, CO_2, SO_2, NO_2, CO, NO, HCl, NH_3, N_2O and CH_4 was performed during experimental runs. In addition, three samples were collected simultaneously for dioxin measurement at three sampling points along the flue duct in each experimental run.

The fuel parameters causing the greatest decrease and increase in PCDD/F formation in this study were the addition of sulphur to the flue gas and increases in the chlorine content of the fuel, respectively. An SO_2:HCl ratio of 0.4 or 1.6 resulted in a 70% reduction of dioxins. An increase from 0.7% to 1.7% chlorine level in the fuel resulted in a ten-fold increase of the dioxin levels. Increasing the temperature of the secondary-combustion zone from 800 °C to 950 °C did not result in a reduction of the PCDD/F level, but a decrease in temperature to 650 °C almost doubled the PCDD/F level. The largest effect on dioxin formation came from transient or incomplete combustion conditions with increased CO levels. No PCDD/F formation was seen at 640 °C, but at 460 °C formation was observed at a level 70% lower than at 400 °C. The greatest rates of formation implied to occur between 400 °C and 300 °C, with indications that the amount and size of particulates were important. The temperature-residence time profiles implied that shorter residence times in this temperature range were associated with lower dioxin levels. These findings were confirmed by multivariate statistical evaluation, using SIMCA-P+ 11.5.

List of abbreviations

APC	Air Pollution Control
CEM	Continuous Emission Monitoring
CV	Coefficient of Variance
dg	dry gas
DIN-PCBs	PCBs 28, 52, 101, 138, 153 and 180
DW	Dry Weight
ESP	Electrostatic Precipitator
FTIR	Fourier Transform Infra-red
GC-HRMS	Gas Chromatography-High Resolution Mass Spectrometry
GC-LRMS	Gas Chromatography-Low Resolution Mass Spectrometry
HCB	Hexachlorobenzene
I-TEQ	International TeCDD-equivalents
MSD	Mass Selective Detector
MSPC	Multivariate Statistical Process Control
MSW	Municipal Solid Waste
MVDA	Multivariate Data Analysis
O-PLS	Orthogonal Partial Least Squares
PCA	Principal Component Analysis
PCB	Polychlorinated biphenyl
PCDD	Polychlorinated dibenzo-*p*-dioxin
PCDF	Polychlorinated dibenzofuran
PCPh	Polychlorinated phenol
PLS	Partial Least Squares
POPs	Persistent Organic Pollutants
PVC	Polyvinyl chloride
RDF	Refuse-Derived Fuel
TeCDD	Tetra-chlorinated dibenzo-p-dioxin
TEF	Toxic Equivalent Factor
UV scaling	Unit variance
CH_4	Methane
CO	Carbon monoxide
CO_2	Carbon dioxide
H_2O	Hydrogen oxide (water)
HCl	Hydrogen chloride
NH_3	Ammonia
N_2O	Dinitrogen oxide
NO	Nitrogen oxide
NO_2	Nitrogen dioxide
O_2	Oxygen
SO_2	Sulphur dioxide

Table of contents

1. Introduction

Dioxins are by-products emitted from combustion sources such as municipal solid waste (MSW) incineration plants. There are substantial environmental concerns regarding these compounds because they are highly toxic and persistent. Dioxins were first detected in MSW ash in 1977 (*1*). The formation of dioxins has been researched for at least 30 years, but although great progress has been made, the mechanisms of formation are still not fully understood. However, dioxins are known to form in the lower temperature region of the post-combustion zone in MSW incineration plants. A significant proportion of dioxins thus formed is associated with fly ash. The most common way to reduce dioxin concentrations in the flue gas is to add activated carbon as a selective dioxin removal step in the flue gas cleaning system, which includes a highly efficient dust removal system. The dioxins can then be destroyed by returning the spent activated carbon to the incinerator. However, this is not possible in a large number of plants because the spent activated carbon is mixed with fly ash, so the dioxins are not destroyed but are retained in the flue gas cleaning residues. Dioxin emissions from MSW incineration have been significantly reduced since they were first detected. The EU Directive on the incineration of waste (Directive 2000/76/EC) (*2*) limits the concentration of dioxins in flue gases to 0.1 ng I-TEQ/Nm^3. In addition, Council Regulation (EC) 1195/2006 amending Annex IV of Regulation (EC) No 850/2004 of the European Parliament and of the Council on persistent organic pollutants limits the dioxin concentration in waste (including residues from waste incineration) to 15 µg I-TEQ /kg (*3*).

The study presented here investigated the effects of varying the combustion parameters on the dioxin contents of the flue gas, and thus the dioxin concentrations in the residual products (bottom ash, boiler ash, fly ash and flue gas cleaning residues). The ultimate aim was to identify combustion conditions that minimize the formation of dioxins during MSW incineration and thus final dioxin levels. A laboratory-scale fluidized-bed reactor was used for this purpose, and parameters such as fuel composition and combustion conditions were varied. Levels of dioxin residues can be reduced either by treating the waste or optimizing the performance of combustion plants. Thermal treatment of ashes or optimization of combustion temperatures, process parameters and fuel composition are the main options. The persistent organic pollutants (POPs) investigated in this study were: polychlorinated dibenzo-*p*-dioxins (PCDDs) and polychlorinated dibenzofurans (PCDFs), polychlorinated biphenyls (PCBs) and hexachlorobenzene (HCB). The study was primarily focused on the PCDD/Fs. The study was performed during three experimental campaigns in spring 2006, autumn 2006 and winter 2007.

2. Background

PCDD/Fs, PCBs and HCB are chlorinated, aromatic compounds with high chemical stability that are, consequently, persistent in the environment. They can also accumulate in the human body due to their lipophilicity (high affinity for fat and low solubility in water).

2.1 PCDD/Fs, PCBs and Chlorobenzenes

Dioxins include two groups of compounds, PCDDs and PCDFs (Figure 1). PCDDs and PCDFs include 75 and 135 different congeners, respectively. Of these 210 compounds, 17 have 2,3,7,8-chlorination patterns, which confer high toxicity (Table 1). 2,3,7,8-TCDD is the most toxic congener of the PCDDs and by definition is assigned a toxic equivalent factor (TEF) of 1 (Table 1). The TCDD-equivalent (TEQ) is obtained by multiplying the concentration of a dioxin congener by its TEF-value and summing the result for all congeners. In this way the dioxin content of a sample that contains many different congeners can be expressed as a single value (I-TEQ) and an estimate of the associated toxicological impact can thus be made. Dioxin concentrations measured in this study were presented as International-TEQs (I-TEQs) using the I-TEF values presented in Table 1.

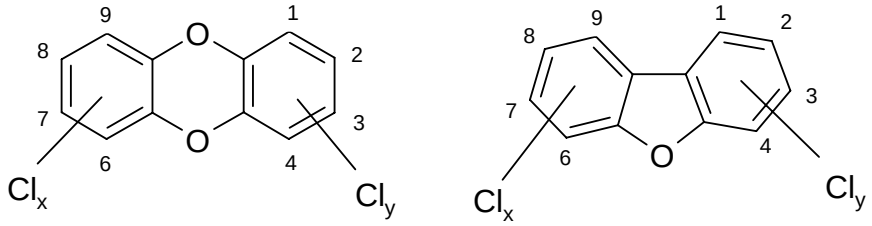

Figure 1. The general structures of PCDDs (left) and PCDFs (right), x and y represent 0-4 chlorine atoms.

Table 1. Toxic equivalent factors (TEFs) (*4*).

PCDDs (Dioxins)	TEF	PCDFs (Furans)	TEF
2,3,7,8-TeCDD	1	2,3,7,8-TeCDF	0.1
1,2,3,7,8-PeCDD	0.5	1,2,3,7,8-PeCDF	0.05
1,2,3,4,7,8-HxCDD	0.1	2,3,4,7,8-PeCDF	0.5
1,2,3,7,8,9-HxCDD	0.1	1,2,3,4,7,8-HxCDF	0.1
1,2,3,6,7,8-HxCDD	0.1	1,2,3,7,8,9-HxCDF	0.1
1,2,3,4,6,7,8-HpCDD	0.01	1,2,3,6,7,8-HxCDF	0.1
OCDD	0.001	2,3,4,6,7,8-HxCDF	0.1
		1,2,3,4,6,7,8-HpCDF	0.01
		1,2,3,4,7,8,9-HpCDF	0.01
		OCDF	0.001

PCBs include 209 different congeners (Figure 2), which can be divided into two groups; planar and non-planar PCBs. The planar PCBs are also referred to as dioxin-like PCBs and have high TEQ values, but usually occur at low concentrations. In this study PCBs are reported as the sum of DIN–PCBs, defined as five times the sum of the DIN-PCB congeners (5) (Table 2), and/or the concentrations of individual planar PCBs (Table 3).

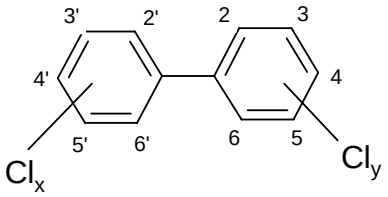

Figure 2. The general structure of PCBs; x and y represent 0-4 chlorine atoms.

Table 2. PCBs included in DIN PCB.

PCB	Congener name
# 28	2,4,4'-Trichlorobiphenyl
# 52	2,2',5,5'-Tetrachlorobiphenyl
# 101	2,2',4,5,5'-Pentachlorobiphenyl
# 138	2,2',3,4,4',5'-Hexachlorobiphenyl
# 153	2,2',4,4',5,5'-Hexachlorobiphenyl
# 180	2,2'3,4,4',5,5'-Heptachlorobiphenyl

Table 3. Planar or dioxin-like PCBs.

PCB	Congener name
# 77	3,3',4,4'-Tetrachlorobiphenyl
# 81	3,4,4',5'-Tetrachlorobiphenyl
# 126	3,3',4,4',5'-Pentachlorobiphenyl
# 169	3,3',4,4',5,5'-Hexachlorobiphenyl

Chlorobenzenes consist of a benzene ring with 1-6 chlorine atoms (Figure 3). Dichlorobenzenes are suspected to cause liver and kidney damage (*6*). In this study the only chlorobenzene reported is HCB.

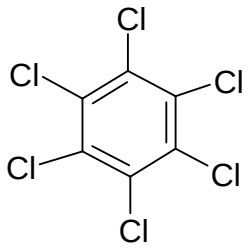

Figure 3. Molecular structure of hexachlorobenzene (HCB).

2.2 PCDD/F formation

The formation mechanisms of PCDDs and PCDFs in combustion processes are very complex and still incompletely understood. The following is an introduction to the proposed reaction pathways and a brief literature study based on laboratory and full-scale investigations.

2.2.1 Reaction pathways

The formation of PCDD/Fs can occur in the gas-phase (homogenous reactions) or on solid phases/surfaces (heterogenous reactions). Gas-phase formation occurs at high temperatures, 500-700 °C. However, according to values calculated by Shaub and Tsang (*7*) gas-phase reactions can only produce very low levels of PCDD/Fs. Accordingly, Vogg and Stieglitz (*8*) found very low concentrations of PCDD/Fs in the gas-phase at 600 °C compared to 300 °C when a stream of air was passed over a MSW ash. Their findings indicated that most formation of PCDD/F occurs on the solid surfaces of MSW ashes in the lower part of this temperature interval, 400-300 °C.

Two reaction pathways have been proposed:

1. *De novo* synthesis, from the elements carbon (C), hydrogen (H), chlorine (Cl) and oxygen (O) (*9*).
2. Formation from precursors such as PCBs, chlorinated benzenes (PCBz) and chlorophenols (PCPh) (*10*).

Both of these pathways occur in the post-combustion zone at temperatures between 250 and 400°C. The PCDF/PCDD ratio is used to discriminate between the two pathways. A PCDF/PCDD ratio >1 is associated with *de novo* synthesis and <1 with formation from precursors (*11*). Generally in MSW incineration the PCDFs levels are 10 times larger than PCDDs levels.

HCl is the most common chlorine source in the flue gas, but it does not act directly as the chlorinating reagent in dioxin formation. HCl must first be converted to Cl_2 (in the gas-phase) (*12*). The theory discussed in the literature is the *Deacon* process (reaction 1) (*12*). In this mechanism, initially proposed by Griffin (*12*) and referred to as the *Deacon* process (reaction 1 below), $CuCl_2$ acts as a catalyst and the optimum temperature is 430 °C (*13*).

$$2HCl + \frac{1}{2}O_2 \rightarrow H_2O + Cl_2 \qquad [1]$$

At the same time that Griffin (*12*) proposed this mechanism he also proposed that dioxin formation could be inhibited by the presence of sulphur dioxide, as illustrated below, (reaction 2). Later the theory of formation of binding the catalyst Cu to $CuSO_4$ has been brought up, reaction 3 (*14*). Scientific opinion diverges on the optimal temperature for reaction 2, which could range from 400 °C (*12*) to 750 °C (*14*). The optimal temperature for reaction 3 is reported to be around 400 °C. However, a full mechanistic understanding of the effect of sulphur on the formation of PCDD and PCDF is still awaited.

$$SO_2 + Cl_2 \rightarrow SO_3 + 2HCl \qquad [2]$$

$$CuO + SO_2 + \frac{1}{2}O_2 \rightarrow CuSO_4 \qquad [3]$$

2.2.2 Effects of fly ash on PCDD/F formation

Since Vogg and Stieglitz found that dioxin formation can occur on the solid surfaces of MSW ash, numerous laboratory-scale studies have been performed using MSW ash. In a recent study by Lundin et al. (*15*) at Umeå University, MSW ash was thermally treated at 300 and 500 °C. The ash was placed in a stainless reactor (diameter 75 mm, length 750 mm) and heated to either 300 °C or 500 °C in air for 30 min. Samples of both the gas-phase and solid-phase were collected, and both thermally treated ash and untreated ash were analysed for PCDD/Fs. The ash treated at 500ºC contained 74% less PCDD/Fs, while ash treated at 300 °C contained 36 times more PCDD/Fs than untreated ash. The dioxin content of the gas-phase from the 300 °C treatment was about 2,000-fold higher than that of the gas-phase sampled at 500 °C. This study showed that PCDD/Fs can be formed from ash when the ash contains appropriate components and the surrounding temperature is within the formation window.

2.2.3 Effects of fuel composition on PCDD/F formation

Chlorine

The effects of the level and source (organic or inorganic) of the chlorine in the fuel have been investigated by Wikström et al. (*16*) at Umeå University, using the same experimental set up as the present project (before renovating and updating it). In their study, polyvinyl chloride (PVC powder) and calcium chloride ($CaCl_2 \cdot 6H_2O$) were used as organic and inorganic chlorine sources, respectively. The total chlorine (Cl) levels in the fuel were 0.12, 0.20, 0.46, 0.56, 0.63, 0.84 and 1.72 % with different ratios of organic/inorganic chlorine contents. A significant increase in PCDD/F formation rate was only observed when the chlorine level in the fuel was 1.72%. The chlorine source (organic or inorganic) did not affect the results. However, the data implied that there is a threshold for the chlorine content of the fuel, above which the dioxin formation rate increases.

Copper

Numerous researchers have shown that copper in the fuel influences the formation of PCDD/Fs (*9,13,17*). In a laboratory-scale fluidized-bed study (combusting model waste) it was demonstrated that copper acts as a catalyst in dioxin formation (0.007%) even when present in low concentrations in the fuel (*18*). When the copper level was increased ten-fold (to 0.07%) the formation of PCDD/F was found to decrease. This was reportedly due to the function of copper as an oxidation catalyst. Copper promoted combustion, *i.e.* the CO concentration in the flue gas decreased with increases in the copper level in the fuel.

Sulphur

Numerous studies involving the addition of sulphur to the combustion zone of MSW incinerators have been performed since sulphur was proposed to be an efficient inhibitor

of PCDD/F formation. For instance, co-firing refuse-derived fuel (RDF) with 5% (w/w) high-sulphur coal in a full-scale plant resulted in a considerable reduction (>70%) in PCDD/F formation (*19*). In addition, in experiments with a laboratory-scale fluidized bed reactor Ogawa et al. (*20*) found that increasing SO_2 levels (from an SO_2:HCl ratio of 0.0004 to 0.1-0.5) resulted in PCDD/F reductions of up to 70%. They also concluded that the addition of coal as a sulphur source had a greater effect than SO_2 on PCDD/F formation. A laboratory scale study by Chang et al. (*21*) indicated that a S:Cl ratio in the fuel of 2 was optimal for dioxin reduction (by about 70%, relative to control levels) and further addition of sulphur did not reduce PCDD/F formation (S:Cl = 3, reduction ca. 30%). However, in Karlsruhe's pilot plant, Tamara, a time delay of several hours was observed before sulphur exerted a detectable effect on PCDD/F formation. This was attributed to deposits of ash on the tube walls remaining from incineration without sulphur addition (*22*). Furthermore, when the addition of sulphur was stopped, the formation of PCDD/Fs increased with incineration time to initial levels. In summary, the addition of sulphur can achieve a 70% reduction of dioxins in the flue gas. The optimal SO_2:HCl ratio for reducing dioxin levels in the flue gas was 0.5, or a S:Cl ratio in the fuel of 2.

Water

The water content of laboratory-scale fuels is lower than that of full-scale plant fuels, giving around 8% and 20% H_2O levels in the flue gases, respectively, and the effects of varying H_2O levels on PCDD/F formation have been investigated at several laboratory scales. Lenoir et al. (*23*) studied the influence of water levels (5, 20 and 25%) on PCDD/F formation in a fluidized bed incinerator (40 kg RDF per hour), and found that water levels had stronger effects (positive correlation) on PCDD formation than on PCDF formation (as did Stieglitz et al., *24*), and no significant effect on total PCDD/F concentrations. However, Jay et al. (*25*) and Ruokojärvi et al (*26*) observed that the presence of water vapour reduced PCDD/F formation in experiments with a micro-scale reactor and a pilot-scale plant (50 kW) burning RDF, respectively. No firm mechanism has been proposed as yet to explain the possible inhibition of PCDD/F formation by water.

2.2.4 Effects of combustion conditions on PCDD/F formation

Combustion variables that have a significant impact on PCDD/F formation parameters include: temperature and residence time in the post-combustion zone; temperature in the secondary-combustion zone, and poor combustion.

Residence times and temperatures in the post-combustion zone

The temperature and residence time (or 'quench time') in the post-combustion zone are considered to be the combustion parameters that most strongly influence PCDD/F formation. The first study to report the dependency of PCDD/F formation on these parameters was performed by Fängmark *et al*. at Umeå University (*27*). Four different post-combustion zone temperatures and three different residence times were investigated: 510, 430, 340 and 260 °C and 0.9, 1.4 and 2.9 seconds. The highest levels of PCDD/F formation were reported to occur at 340 °C with a residence time of 2.9 seconds, and the lowest at 260 °C with a residence time of 0.9 seconds. This study used an earlier version

of the laboratory-scale fluidized-bed reactor than that used in the present project. It should also be noted that the reactor used in the studies presented here has been significantly updated from the former versions used by Fängmark.

High temperature formation – gas-phase formation
High temperature (>650 °C) formation of PCDD/Fs has been examined in few studies, although it has been reported by Wikström et al. (*28*) from Umeå University, Hatanaka et al. (*29*) and Blumenstock et al. (*30*). The study by Wikström et al. used the same experimental set-up as to the present study, however not updated as the present. Sampling was performed at 650 °C at sampling port P2 and 200 °C at sampling port P7 (Figure 4, below). At 650ºC the concentration of PCDD/F in the flue gas was about 50-fold lower than at 200 °C (*28*).

Secondary-combustion temperature and residence time also affect the completion of combustion reactions, e.g. oxidation of CO to CO_2. For optimal oxidation the temperature should be 800-900 °C and the residence time should be about 2 seconds (*31*). A study by Hatanaka et al. (*29*) investigated the formation of PCDD/F between 700 and 900 °C in the secondary-combustion zone, using a laboratory-scale fluidized-bed reactor. Sampling was performed at the end of the secondary-combustion zone. The study showed that PCDD/F concentrations decreased with increases in temperature in the secondary-combustion zone, that the decreases were greatest between 700 and 800 °C and that the temperature changes most strongly affected the PCDFs.

Oxygen level in the flue gas and transient combustion conditions
Increases in oxygen levels (from 1% to 4% and 10%) have been found to increase PCDD/F formation (*32*). However, reductions in O_2 levels during combustion could lead to increased CO concentrations (CO-peaks), due to incomplete combustion. PCDD/Fs are well known to be products of incomplete combustion, and numerous researchers have reported that or transient combustion conditions can lead to increased rates of PCDD/F formation (*30,33-37*). Transient combustion conditions occur not only during malfunctions in the system, but also during start-ups and shut-downs of MSW incinerator plants. Transient conditions also can cause elevated PCDD/F levels for a time following disturbances, referred to in the literature as ‘memory effects’. Two different memory effects are often discussed: *de novo based memory effects* and *adsorptive memory effects* (*36*). The former are associated with deposits of carbon structures in the higher temperature zone of the cooling section, while the latter occur in parts of the lower temperature zone of the cooling section, such as wet scrubbers and electrostatic precipitators (ESPs), in which PCDD/Fs have already been formed and are slowly ‘bleeding’ from the wall surfaces. Neuer-Etscheidt et al. (*38*) found increased PCDD/F concentrations in the ESP ash (but not in the boiler ash), due to transient combustion conditions in a full-scale plant they examined.

3. Materials and Methods

3.1 Experimental set-up

The experiments in the present study were performed using Umeå University's 5 kW laboratory-scale fluidized-bed reactor, which was originally constructed in 1994 to simulate the behaviour of a full-scale waste incinerator (Figure 4), and was described by Wikström et al. in 1998 (*39*), although modifications were made in 2005. Briefly the reactor consists of a bed section (primary-combustion zone one), freeboard (secondary-combustion zone), a convector section (post-combustion zone) and an air pollution control system (APC). The APC system consists of a cyclone (A), a metal and textile filter (B), a wet scrubber (C), and an active carbon filter (D) (Figure 4). The bed and freeboard sections are constructed of a FeCrAl tube, operating temperature up to 1400 °C. The duct connecting the freeboard to the convector is made of 253MA grade stainless steel (operating temperatures up to 1150 °C), and the tubes in the convector section are made of titanium-stabilized stainless steel suitable for operating temperatures <850 °C.

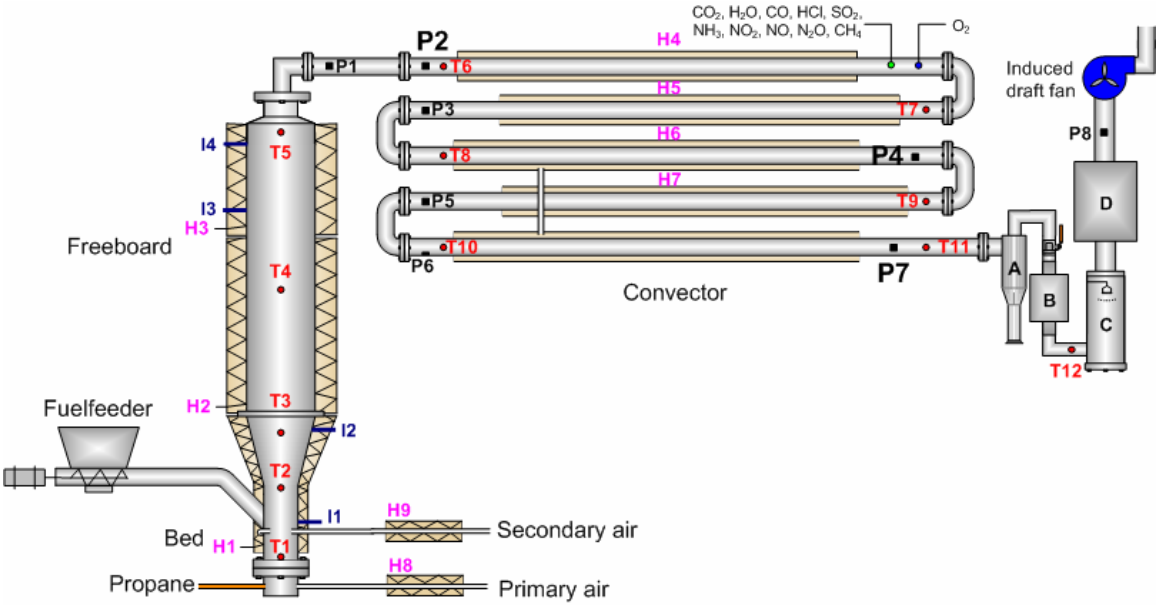

Figure 4. Schematic diagram of the laboratory-scale fluidized-bed reactor (not to scale). Sampling ports are denoted P1-P8, electrical heaters H1-H9, thermocouples T1-T12, and injection ports I1-I4. The FTIR gas analyzer and oxygen probe are connected to the end of the first convector section. Particulate matter sampling was performed at P4.

Six hundred grams of washed sea sand (Barskarpsand 15), sieved to a size range of 125-250 μm before use, were used in the fluidized bed. The fluidized-bed was fed with a solid fuel, which is described in section *3.2, Fuel composition and additives*. The fuel feeder was constructed with a screw and vibrator and was connected to the bed zone by a plexiglass tube containing a v-shaped chute, which substantially improved the evenness of the fuel feed compared to the fuel feed used before the modifications, in the studies by Wikström referred to above. The primary and secondary air inlets had maximum settings of 120 and 100 L/min, respectively. The secondary air was preheated, using a heating-jacket, to about 250 °C before being introduced to the bed. The reactor required pre-

heating before solid fuel incineration started. This was achieved by combusting propane (3.7 L/min) for two hours.

For a small scale reactor, external heat is required to reach temperatures similar to those of full-scale plants. For this purpose, one heating-jacket was used in the bed section and two in the freeboard. Measurements at T4 and T5 showed the flue gas temperature in the freeboard to be steady, after equilibration. Parts of the tubes in the convector section were double-cased to allow the convector section to be heated using hot air. The whole reactor was insulated by wrapping it in ceramic fibre. Drops in temperature occurred at each of the 180° bends connecting the convector units. At the first two bends the temperature drop was about 60 °C and in bends three and four the temperature drop was around 40 °C. The thermocouples (12 N-type sheathed) were mounted directly into the flue gas duct, which is another modification from the configuration used by Wikström. With these heating arrangements both the freeboard and the convector temperatures can be varied easily. Thus, samples of flue gases representing various combinations of temperatures and residence times can be collected for dioxin analyses.

Four different injection ports were available for supplying liquid or gas additives in the bed or freeboard. In the present study, a Brooks SHO-RATE model R-2-15-C flow meter calibrated for 2% SO_2 was used to inject the SO_2 gas through injection port 1 (I1) into the combustion zone. The SO_2 was pre-heated to ca. 250 °C by a small heating jacket before injection into the combustion zone. A peristaltic pump (Alitea Speed Control) was used for adding liquid water (H_2O), also through I1. A connecting tube between the pump and the combustion zone was heated by conduction from the combustion zone and worked similarly to a carburettor in vaporising the liquid H_2O.

The reactor was monitored using the Windows-based program LabVIEW 7.1. The temperatures, air flow and fuel feed were logged every 15 seconds. Continuous emission measurements (CEMs) were performed with an ABB Bomem 9100 Gas Analyzer, based on a Fourier-Transform Infra-red (FTIR) spectrometer and a ScanTronic OC 2010 oxygen measurement probe with a zirconium dioxide (ZrO_2) cell. The FTIR measured H_2O, CO_2, SO_2, NO_2, CO, NO, HCl, NH_3, N_2O and CH_4 once every 30 seconds, on average, and the ZrO_2 cell measured O_2 every second. The CEM analyzers were new and different from the CEM equipment used by Wikström and Fängmark.

The flue gases were drawn through the system by a single inlet, directly driven centrifugal radial fan (MPT 03T, supplied by Ventur Tekniska AB). The maximum flow rate and pressure were 410 m^3/h and 1150 Pa, respectively. A differential pressure transmitter located in convector unit number two measured the negative pressure of the flue gas and controlled the induced draft fan automatically. The reactor was checked for leaks before each experimental campaign, by adding nitrogen (N_2) via injection port 1 (I1) and measuring the O_2 level under negative reactor pressure.

3.2 Fuel composition and additives

The fuel used was an artificial municipal solid waste (MSW) made at Umeå University, with a composition based on typical, or 'average' Swedish MSW (*40*), as shown in Table

4. The ingredients were homogenised and the mixture was compressed into pellets, with a diameter of 6 mm and length of 10-30 mm. The elemental content, dry weight, ash content and heating value of the pellets were determined, and are listed in Table 5. The elemental content and heating value were determined by an accredited laboratory at SLU (Swedish University of Agricultural Sciences). Inorganic analyses were conducted by Analytica AB in Luelå, Sweden (again, an accredited laboratory). In total, chlorine accounted for 0.7% mass of the fuel (0.27% inorganic and 0.43% organic, the latter consisting of PVC).

Table 4. Ingredients of the artificial MSW waste.

Material	***Percentage (w/w)***
Paper confetti	36.0
Wheat starch	15.5
Sawdust	10.5
Polyethylene	10.5
Gelatine	7.5
Peat	5.0
Rapeseed oil	5.0
Silica gel (SiO, ∅0.6-0.2 mm)	3.0
Sand (∅150-250 μm)	2.5
Kaolin ($Al_4OH_8SiO_{10}$)	1.7
Iron powder (Fe)	1.2
Polyvinyl chloride powder (PVC)	0.8
Calcium chloride ($CaCl_2 \times 6H_2O$)	0.7
Copper acetate ($CuO_4C_4H_6$)	0.02

Advantages of using an artificial MSW include fuel homogeneity and accurate knowledge of its composition. Calculating the elemental composition of the ash/solid phase in the flue gas is therefore straightforward and the composition of the fuel is easy to vary according to the purpose of the combustion experiments.

Two additional, smaller batches of fuel were made for the experimental runs 17 and 18 (Table 6). For experimental run 17 the chlorine level was increased to 1.7% (compared to 0.7% in the starting fuel), by increasing both the PVC and calcium chloride content 2.5-fold. The proportions of inorganic and organic chlorine in this batch (run 17) were 0.67% and 1.03%, respectively. For run 18 the copper level was increased two-fold relative to the starting fuel, by adding twice as much (0.04%) copper acetate to the fuel mix. However, the copper level measured in the fuel was 0.011% (not twice the amount). The results of analyses of these two smaller batches of fuel showed only minor differences in the levels of other components compared to the start fuel.

The sulphur level in the fuel showed to be low. This could be due to a low level of sulphur in the peat. In two experimental runs (19 and 20) sulphur was added to the combustion zone as sulphur dioxide (SO_2). The total (fuel-sulphur and SO_2) sulphur level

in the fuel, calculated from the sulphur concentration added and the fuel feed rate, for experimental runs 19 and 20 was about 1.9% and 3.9%, respectively. The sulphur:chlorine ratios (on a molar basis) in the fuel for the two runs were 1.6 and 3.1.

The dry weight of the fuel was 95%. This dryness was needed to form pellets. Water (H_2O) was added at a rate of approximately 0.90 l/hour into the combustion zone in experimental run 21.

Table 5. Elemental composition of the artificial MSW fuel

Element	Unit	Level
Dry weight (DW)	%	95
Ash content	%	18
Heating value, calorimetric	MJ/kg DW	19.3
Copper	% of DW	0.007
Sul**ph**ur	% of DW	0.07
Chlorine	% of DW	0.7
Carbon	% of DW	44.8
Hydrogen	% of DW	6.3
Nitrogen	% of DW	1.4
Oxygen	% of DW	30.6
Silicate (SiO_2)	% of DW	6.6
Al_2O_3	% of DW	0.7
Na_2O	% of DW	0.07
TiO_2	% of DW	0.007
K_2O	% of DW	0.05
CaO	% of DW	3.8

3.3 Experiments

Twenty-three experimental runs were performed with 14 variants of conditions, some of which were performed in two, three or even five replicates (Table 6) and, in total, 78 dioxin samples were obtained. The reproducibility of the experimental set-up was evaluated by performing five experimental runs using the same target combustion parameters (Table 7). These runs are henceforth referred to as baseline runs or baseline. Five baseline runs were performed because there were three different experimental campaigns.

The baseline runs were intended to establish similar operating conditions with respect to the following parameters: flue gas temperatures in the bed, freeboard and convector sections; residence time in the post-combustion zone; oxygen (O_2) level in the flue gas; H_2O level in the flue gas; efficiency of combustion with respect to the carbon monoxide (CO) level in the flue gas, and fuel load (Table 7). The particulate matter (PM) in the flue gas was also a parameter of interest, but this depended on the fuel load and a target value was not therefore set. Residence time in the post-combustion zone was defined as the time the flue gas took to travel from the beginning of the post-combustion zone to the

sampling port, calculated from the elemental content of the fuel, air supply, local temperatures and volume of the laboratory-scale reactor. The air supply settings in runs 1-5 (baseline runs), 6-14 and 17-21 were 110 L/min of primary air and 30 L/min of secondary air. Settings for the runs 15, 16, 22 and 23 are shown in the experimental descriptions below.

Table 6. Experimental matrix.

Run	Experiment	Description	Sampling temperatures [°C]	Sampling ports
1	Baseline	See table 7.	640, 300, 200	P2, P4, P7
2	Baseline	repeat 1	640, 300, 200	P2, P4, P7
3	Baseline	repeat 1	640, 300, 200	P2, P4, P7
4	Baseline	repeat 1	400, 300, 200	P3, P4, P7
5	Baseline	repeat 1	400, 300, 200	P3, P4, P7
6	High temperature in the convector	Maximum effect of H4-H7 = minimum cooling rate	460, 360, 260	P3, P4, P7
7	High temperature in the convector	repeat 6	460, 360, 260	P3, P4, P7
8	High temperature in the convector	repeat 6	460, 360, 260	P3, P4, P7
9	Low temperature in the convector	Minimum effect of H4-H7, = rapid cooling rate	640, 200, 100	P2, P4, P7
10	Low temperature in the convector	repeat 10	640, 300, 200	P2, P4, P7
11	Temperature changes in the convector	Increased effect of H6 = slowed cooling rate	400, 333, 300	P3, P4, P6
12	Temperature changes in the convector	repeat 11	400, 333, 300	P3, P4, P6
13	Reduced temperature in the freeboard	660°C in the freeboard (T4 and T5)	640, 300, 200	P2, P4, P7
14	Increased temperature in the freeboard	950°C in the freeboard (T4 and T5)	640, 300, 200	P2, P4, P7
15	Reduced fuel load	0.68 kg/h or 3.6 kW	640, 300, 200	P2, P4, P7
16	Reduced fuel load	0.60 kg/h or 3.2 kW, repeat 15	400, 300, 200	P3, P4, P7
17	Increased Cl-level in the fuel	Cl-content: 1.7 % DW in the fuel	400, 300, 200	P3, P4, P7
18	Increased Cu-level in the fuel	Cu-content: 0.011 % DW in the fuel	400, 300, 200	P3, P4, P7
19	Addition of SO_2	1.9% in the fuel[a]	400, 300, 200	P3, P4, P7
20	Addition of SO_2	3.9% in the fuel[a]	400, 300, 200	P3, P4, P7
21	Addition of H_2O	Addition of 0.9 L/min,	640, 300, 200	P2, P4, P7
22	Reduced O_2-level in the flue gas	Injection of N_2 – propane inlet	640, 300, 200	P2, P4, P7
23	Reduced O_2-level in the flue gas	Injection of N_2 – I1	400, 300, 200	P3, P4, P7
3B	Transient conditions	Increase in CO concentration	640, 300, 200	P2, P4, P7
3C	Memory effects 1	Steady state	640, 300, 200	P2, P4, P7
3D	Memory effects 2	Steady state	640, 300, 200	P2, P4, P7

[a] Calculated value from the sulphur concentration added and the fuel feed rate.

Table 7. Target values for the baseline runs.

Combustion parameter	Target value	Residence time [seconds]
Bed [°C]	800-850	
Freeboard[a] [°C]	800	5.1[d]
P2[b] [°C]	600	0.1[e]
P3[b] [°C]	400	1.4[e]
P4[b] [°C]	300	2.3[e]
P7[b] [°C]	200	4.4[e]
H_2O [vol%]	8-9	
O_2 [vol% dg]	10-11	
Excess air ratio (λ)	1.9	
CO [ppm dg]	<10	
Fuel load [kg/hour]	0.93	
Fuel load [kW]	5.0	
PM[c] [mg/Nm^3 dg 11% O_2]	1200	

[a] Freeboard temperature at T4 and T5.

[b] Temperature at sampling port in the convector section.

[c] Particulate matter, average value of the basal runs 2-5.

[d] Residence time in freeboard.

[e] Accumulated residence time in post-combustion zone.

The parameters varied in the experiments were related to both fuel and combustion conditions. Three variants were performed with different temperatures at the sampling points of the post-combustion zone from those used in the baseline runs. In experimental runs 6-8 heating of the post-combustion zone was set to maximum, thereby slowing the rate of cooling. This resulted in the temperatures at the sampling points P3, P4 and P7 being 460, 360 and 260 °C respectively. For experimental runs 9 and 10 the post-combustion zone external heating was low. The temperatures at sampling points P3, P4 and P7 were 300, 200 and 100 °C, respectively. Only a small change in the convector temperature profile was made for runs 11 and 12. The temperatures at the sampling points P3, P4 and P5 were 400, 333 and 300 °C (sampling point P5 was used instead of P7), respectively. The flue gas residence time in the post combustion zone was also modified for runs 11 and 12. Figure 5 illustrates the residence time and temperature profiles in the post-combustion zone for runs 1-12.

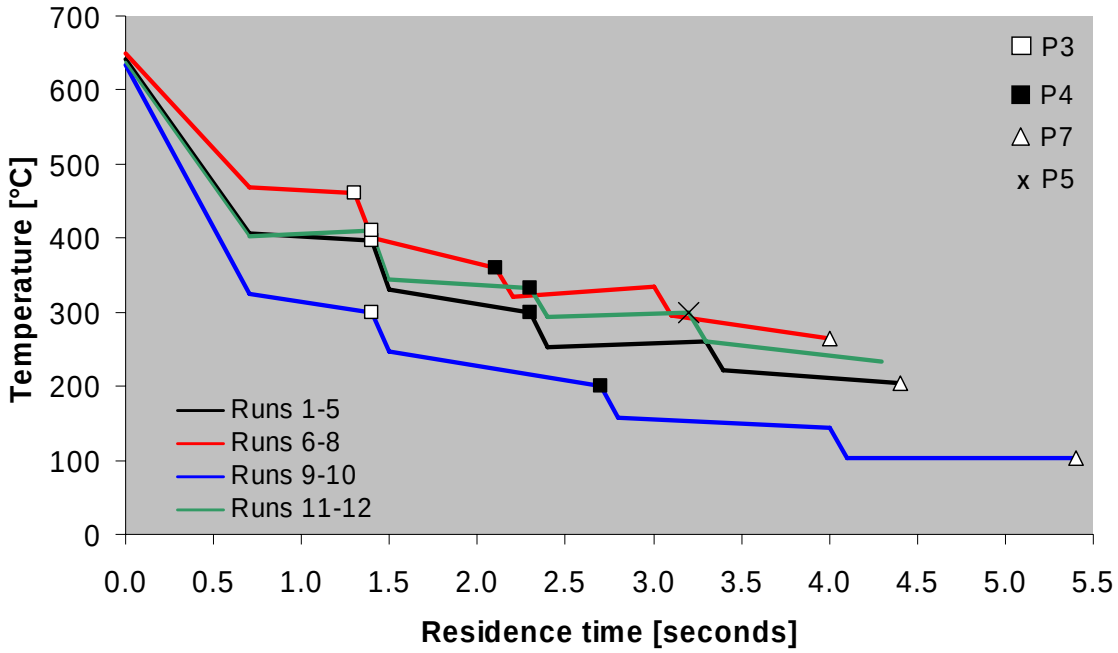

Figure 5. Temperature-residence time profiles investigated in the post-combustion zone. The sharp drops are due to heat losses in the bends of the convector tubes (no external heating).

In runs 13 and 14 the freeboard temperature was varied. In experimental run 13 the heating system of the freeboard was turned off, resulting in the temperature being 660 °C (at both T4 and T5). For run 14 the heating system was set to 950 °C in the freeboard, 150 °C higher than in the baseline runs. The residence time in the freeboard was altered in these two runs to 5.9 (run 13) and 4.5 seconds. The residence time in the freeboard for the baseline runs was 5.1 seconds. For these runs only minor alterations were observed in the temperature-residence time profile in the post-combustion zone. The sampling points used in these experiments were P2, P3 and P7.

In experimental runs 15 and 16 the fuel load was reduced. The fuel feed rate was reduced to approximately 0.63 kg/h compared to about 0.92 kg/h in the baseline runs. The air supply was adjusted to 74 L/min and 22 L/min from the primary and secondary air inlets, respectively. The excess air ratio was thus maintained as for the baseline runs. However, the residence times in the freeboard and post-combustion zone were increased. The sampling points used in experimental run 15 were P2, P3 and P7, while P3, P4 and P7 were used in experimental run 16. It should be noted that experimental run 15 was performed in a separate experimental campaign prior to those referred to in the present study.

In five experiments (runs 17-21) the effects of changes in the fuel composition were investigated, either by adding elements to the fuel or injecting additives to the combustion zone. In experimental runs 17 and 18 the copper and chlorine levels were increased, respectively. The copper level in the fuel for run 17 was 0.011% (compared to 0.007% in baseline runs), and the chlorine level was increased from 0.7% to 1.7% in the

modified fuel used in run 18. For experimental runs 19 and 20, SO_2 with a concentration of 2% was added through injection port 1 (I1) into the combustion zone in order to obtain 100 and 500 ppm SO_2 in the flue gas, respectively. In experimental run 21, H_2O was added through injection port 1 (I1) into the combustion zone to increase the H_2O level in the flue gas to a level similar to that in full-scale plants. The changes made to the fuel and the additives used are discussed in detail in section *3.2 Fuel composition and additives*. The sampling points used in experimental runs 18 and 21 were P2, P3 and P7 and in experimental runs 17, 19 and 20 points P3, P4 and P7 were used.

For the last two experimental runs (runs 22 and 23) the O_2 level was reduced in the flue gas by adding nitrogen (N_2) to the combustion zone (in order to maintain the same residence times in the freeboard and convector), through the propane inlet in experimental run 22 and at I1 in experimental run 23. In run 22 the primary air supply was reduced to 40 L/min and complemented with 40 L/min of N_2. In run 23 the primary air supply was reduced from 110 L/min to 90 L/min. The secondary air supply (previously 30 L/min) was changed to 50 L/min of N_2. N_2 was added at I1 in run 23 to obtain the same CO level as in run 3B and the same O_2 level as in run 22. The sampling points used in experimental run 22 were P2, P3 and P7 and in experimental run 23 points P3, P4 and P7 were used.

Run 3 lasted for nine hours in order to evaluate transient combustion conditions (Figure 6). Sampling was performed on four occasions during the run:

1. Good combustion (3)
2. Transient combustion (3B). The CO level was increased by adding more fuel and reducing the air supply, giving CO-peaks >3000 ppm every third minute for one hour. Sampling was performed during 30 min.
3. Memory effects 1 (3C). Sampling started directly after the transient combustion period and was performed during 30 min.
4. Memory effects 2 (3D). Sampling started 60 minutes after the transient combustion period and was performed during 30 min.

The other experimental runs each required five hours of MSW combustion. Dioxin samples were collected at three sampling points along the flue duct simultaneously during a single 45-minute period, after four hours of MSW combustion (Figure 7). Sampling points for each experimental run are recorded in Table 6. Particulate matter was sampled after 2 hours of MSW combustion at sampling port P4. CEM was performed during the entire experimental runs. After each experimental run the fuel feed was turned off and the air supply was set to 50 L/min for overnight cooling of the reactor. The ashes left in the reactor (the bottom, convector and cyclone ashes) were collected and saved from each experimental run. The proportions of these ashes were calculated by dividing the amounts of ash left in the bed, convector and cyclone by the total amount of ash collected, and the total ash content was calculated by dividing the total amount of ash by the total amount of fuel loaded into the reactor. The resulting figures were used to obtain an understanding of the system. The total ash content was therefore different from the ash content determined from analysis of the fuel (Table 5). The minor differences were due to practical handling

of the ashes during collection, *i.e.* some ash tended to fly away. After each experimental run the reactor was thoroughly cleaned, the freeboard was swept and the convector was cleaned with compressed air and vacuumed.

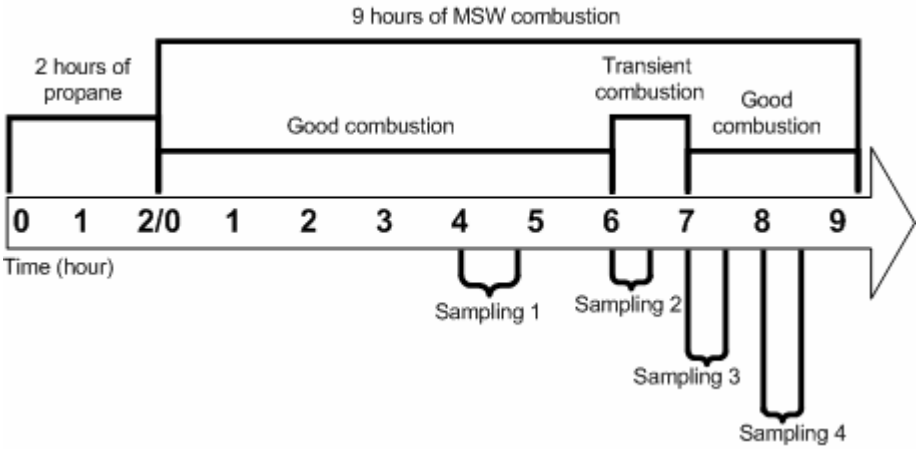

Figure 6. Timeline of experimental run 3.

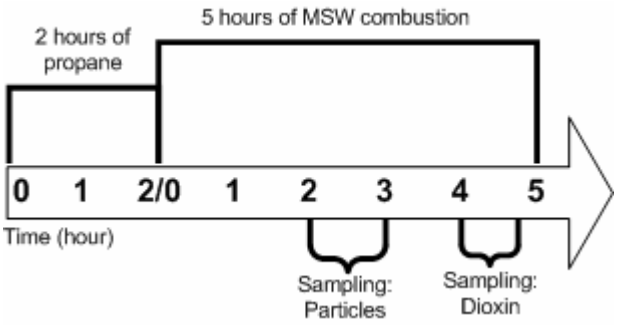

Figure 7. Timeline of experimental runs 1, 2 and 4-23.

3.4 Sampling

Dioxin sampling was performed isokinetically, *i.e.* at the same velocity as the velocity of the flue gases in the duct, to ensure that the particle size distributions in the samples were the same as in the flue gas. Dioxin sampling of the flue gases was conducted using the cooled probe polyurethane foam plug (PUFP) sampling technique, according to European standard EN-1948:1 (*41*). The sample train consisted of two glass flasks, one containing water and the other containing ethylene glycol (Figure 8). On the top of the ethylene glycol flask were two PUFPs with a glass microfibre filter between them. The particles were collected in the flasks and the aerosols were collected in the filter. Before sampling, $^{13}C_{12}$-labeled sampling standards (SS) of PCDD/Fs and PCBs were added to the water flask in the sample train. These standards were used to check for losses of PCDD/Fs during sampling, transport and storage. The glass probe inside the cooled probe was made of either pyrex glass, quartz glass or titanium. For sampling temperatures 100-400 °C, pyrex glass was used. Quartz glass probes were used for sampling at 460 °C and a titanium probe was used for sampling at 650 °C (only in the third experimental campaign). When sampling from a full-scale plant, part of the cooled probe is placed

inside the flue gas duct. For the small flue gas duct (convector) used in this study, only the nozzle of the probe was placed inside the duct (Figure 8), in the middle of the flue gas stream. For sampling at 460 °C and 650 °C another cooled probe was placed outside the existing water-cooled probe. This outer probe was filled with a mixture of ice and salt (NaCl) to maintain a temperature of -12 °C. The temperature outside the glass/titanium probes after cooling was ca. 20 °C during flue gas sampling.

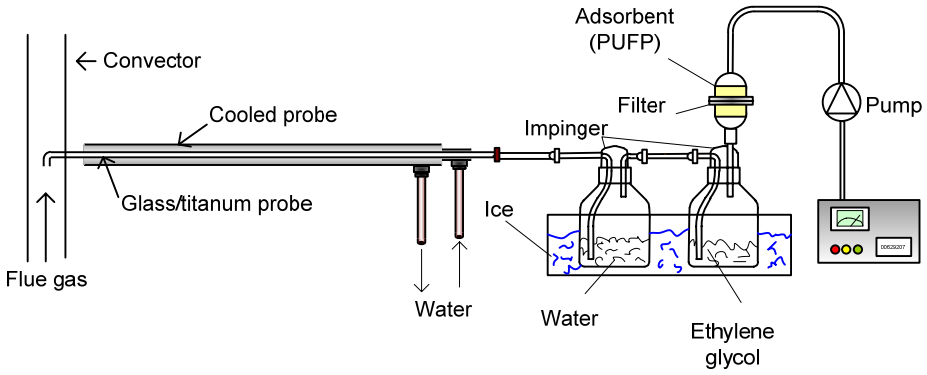

Figure 8. Sample train with cooled probe. The cooled probe **was perpendicular** to the sample train in all sampling that was performed, except for sampling at 460 and 650 °C.

To ensure that there were no leaks in the sample train, the filter holder was checked before sampling. Also, during sampling the O_2 level was measured in the exhaust gas from the pump and compared to the O_2 level in the flue gas. A higher O_2 level in the pump exhaust than in the flue gas would thus indicate a leak. After sampling the probe was rinsed with water to collect condensate from the probe wall. This rinse was collected and added to the water flask. The probe and the impingers were rinsed with toluene into a separate bottle. A new glass probe was used for each sampling event. The probes were cleaned with toluene and acetone before use and the titanium probe was heated to 550 °C for 6.5 hours. A field blank (consisting of sample equipment but no sample) was performed in each experimental campaign. The pumps used to draw the flue gas out were calibrated with a gas meter before and after each experimental campaign. The gas meter was calibrated every other year by the SP Technical Research Institute of Sweden.

Particulate matter (PM) was sampled isokinetically using an STL Combi dust sampler (Metlab, Sweden), which adsorbed particles on preheated (about 120 ºC) quartz filters, according to Swedish Standard method EN 13284-1 (*42*) (Figure 9). The sampler consisted of two quartz filters. The filters were pre-heated to 120 °C with hot air for one hour before sampling and heating was discontinued when sampling commenced. Before sampling the quartz filters were heated overnight in an oven, cooled in a dessicator and finally weighed. After sampling the same procedure was performed. PM concentrations were normalised (Nm^3): to 1013 h Pa, 273 K, dry gas (dg) and 11vol-% O_2.

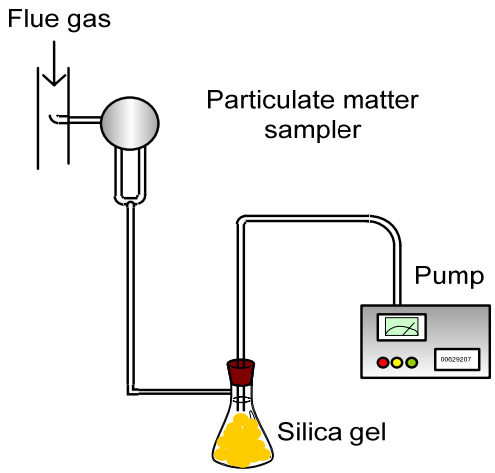

Figure 9. Particulate matter sampling. The silica gel was used to **remove** condensed water before the gas entered the pump.

3.5 Extraction, clean-up and analysis of PCDD/Fs, PCB and HCB

Figure 10 presents a flow chart of the sample treatment steps in the laboratory. Before extracting the samples, additional $^{13}C_{12}$-labeled internal standards (IS) were added to the water flask to compensate for losses during extraction and clean-up. The ethylene glycol and water were combined and filtered twice. In the first filtration a glass fibre pre-filter and a membrane (0.45 µm) filter were used to adsorb particles. The second filtration collected organic substances using a solid-phase extraction disk (Envi-disk). All the glassware was rinsed with toluene and added to the bottle containing the probe rinse. The filters, PUFPs, glass microfibre filter and the toluene from the glassware rinse were extracted overnight under reflux using a Soxhlet-Dean-Stark apparatus. A laboratory blank, subject to all of the above steps, was included to ensure the quality of the analyses. All the glassware used in the sample train was washed, heated at 550 °C for 6.5 hours, washed with toluene and acetone and finally wrapped in aluminium foil before use.

Each sample extract was evaporated to a volume of a few millilitres, then divided into three portions by volume: 50% for PCDD/F and PCB clean-up, 25% for HCB clean-up and 25% was retained. Clean-up was performed according to standard methods (*43*) that are described briefly below.

For PCDD/Fs and PCBs the extract was applied to a multisilica-column, eluted with hexane onto an alumina column and eluted with dichloromethane:cyclohexane. The eluted fraction was evaporated to a few millilitres. The sample was applied to a carbon:celite-column, eluted first with *n*-hexane and then with a mixture of dichloromethane:*n*-hexane to collect the PCBs. Finally the carbon:celite-column was eluted with toluene to collect the PCDD/Fs (in a separate flask). A $^{13}C_{12}$-labeled recovery standard (RS) and tetradecane (keeper) were added to each of the fractions (PCDD/Fs and PCBs). The RS was used to calculate the losses during extraction and clean-up, and the keeper to ensure that PCDD/Fs and PCBs would not be lost during final evaporation. The sample was evaporated to 40 µl. For HCB clean-up the sample was applied to a deactivated silica column and eluted with cyclopentane. RS and toluene (keeper) were

added to the sample. The sample was evaporated to a volume of 0.5 ml. A clean-up blank was processed to ensure the quality of the analyses.

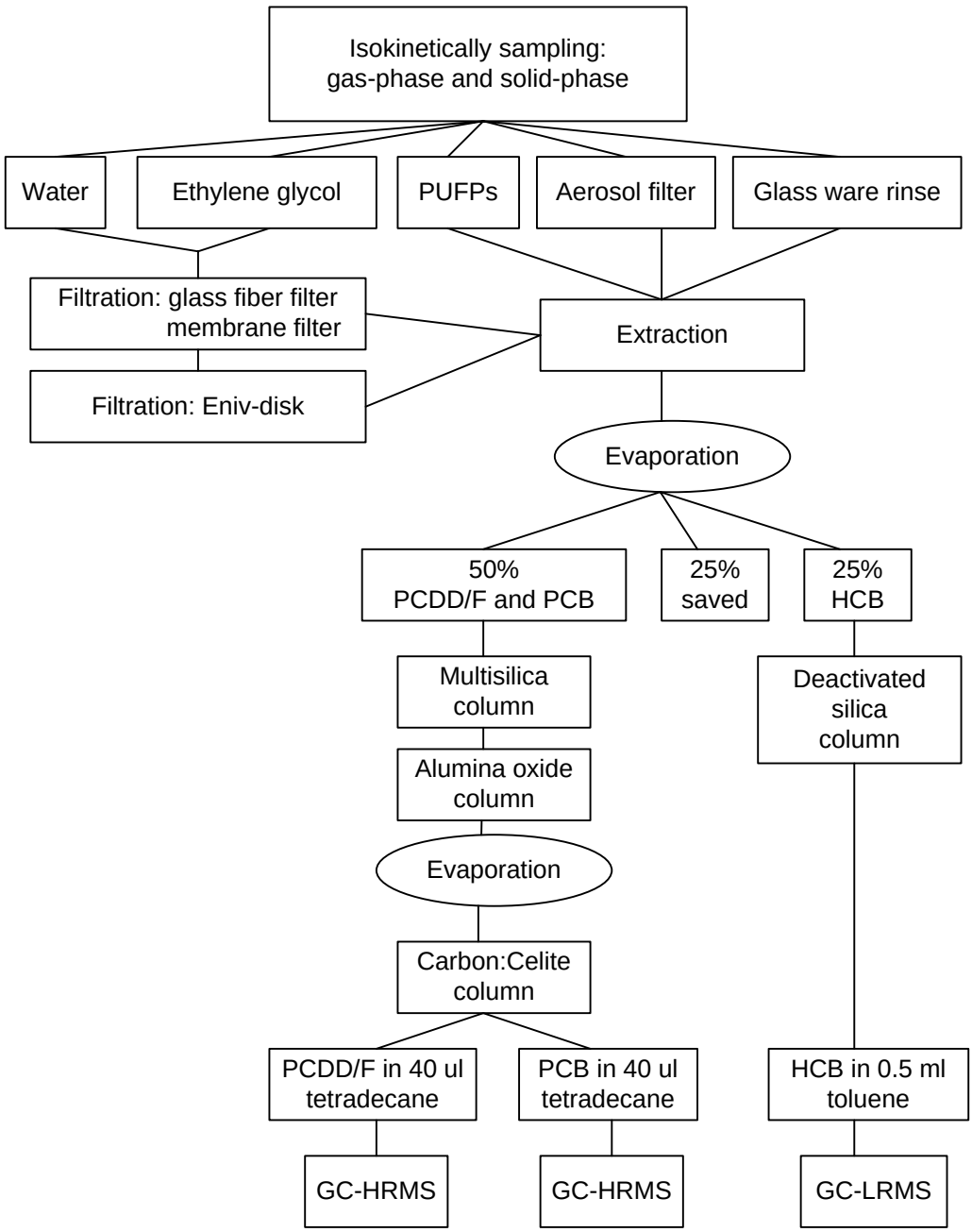

Figure 10. Flow chart of sample treatment steps in the laboratory.

A portion (3 µl) of the 40 µl final volume of the PCDD/F or PCB extract was analysed by GC-HRMS using a Waters AutoSpec ULTIMA NT 2000D high resolution mass spectrometer fitted with a 60m×0.25mm×0.32 µm J&W Scientific DB-5MS column. A portion (2 µl) of the 0.5 ml final volume of the HCB extract was analysed by GC-LRMS using an Agilent 5975 MSD low resolution mass spectrometer equipped with a

30m×0.25mm×0.25 µm J&W Scientific DB-5MS column. PCDD, PCDF, I-TEQ, PCB and HCB concentrations were normalised to standard conditions (Nm^3): 1013 h Pa, 273 K, dry gas (dg) and 11vol-% O_2.

3.6 Multivariate Data Analysis

Multivariate data analysis (MVDA) was applied, using the Windows-based software SIMCA-P+ 11 and 11.5, to investigate correlations/relationships between the varied parameters and the formation of PCDD/Fs, PCBs and HCB. The objective was to identify the parameters with the greatest influence on PCDD/F formation. MVDA was also used to evaluate the stability of the combustion process.

Before using the software a large data table was constructed. Each row represented a discrete sample (*e.g.* baseline run 1, sampling point P4) and each column represented a different parameter (*e.g.* sampling temperature, SO_2, O_2, PCDD concentration). Because different units were used in the table (*e.g.* °C, ppm, %, ng/Nm^3) the data were scaled using *unit variance (UV) scaling*. That means that each parameter was of equal importance and all parameters made an equal contribution to the model.

The MVDA contains a large amount of points in a high-dimensional space. These points were converted to a plane, which was made with a multivariate projection method. SIMCA-P+ 11.5 use the methods: principal component analysis (PCA), partial least squares (PLS) and orthogonal partial least squares (O-PLS). The principal of PCA, PLS and O-PLS are fully described elsewhere (*44-46*). Briefly the PCA uses the whole table as an X matrix. While PLS and O-PLS sets the parameters varied (*e.g.* sampling temperature, SO_2, O_2) in the table as the X-matrix, and the result of the samples (*e.g.* PCDD concentration) as the Y-matrix. In this study O-PLS was used, which is a modification of the original PLS model. The O-PLS separates the data in the model better than PLS. That is, the result from the model is easier to interpret. The projected plane consists of two principal components: PC1 and PC2. The model can make more PCs, which could improve the description of the model. It is not recommended to make more than 4.

The data obtained from the O-PLS model were described in two types of plots, called S*core plots* and *Loading plots*:

- The S*core plot* showed how the samples were distributed and related to each other. Two score plots were made, in the first plot PC1 was plotted against PC2 and in the second plot PC2 was plotted against PC3. Hotellings T^2 was used to define a 95% tolerance area. Samples close to the centre (origin) of the plot were an indication of being an average value. That is, they had same parameters with similar influence on the model. Samples located separate from the other samples had one or more parameters that had a divergent influence on the model. Samples close together, which were making groups, had the same parameter that had a divergent influence on the model. Samples outside the tolerance area are called outliers. These outliers would have one or more parameters with a very divergent influence on the model. Samples on the margin of the area were called moderate

outlier. To establish which parameters that influenced the samples, the loading plot was necessary.

- *Loading plots* show how the parameters are distributed and related to each other. As for the score plots, two loading plots were made: PC1 versus PC2 and PC2 versus PC3. A parameter close to the origin has weak influence on the model while those further from the origin have a strong influence on it. Parameters that are close together contribute similar information about the model. Parameters that are placed on opposite sides of the origin, either vertically or horizontally, are negatively correlated.

The score and loading plots should be interpreted together. For example, a sample located on the upper right hand side of the score plot would be most influenced by parameters located on the upper right hand side of the corresponding loading plot.

Diagrams called S*core contribution plots* provide further information about the results, indicating which parameters contribute the most to the average sample in the model. Contributions have a negative or positive value, indicating whether the parameter has a value smaller or greater than the average sample in the model. Combined interpretation of score/loading and score contribution plots can identify the parameters with the greatest influence on PCDD/F, PCB or HCB formation. In order to determine if an identified parameter tends to increase or decrease formation of the compounds, the concentrations in the samples are read from the table of results.

Multivariate statistical process control (MSPC) based on PCA was used to evaluate the stability of the combustion process. This evaluation was based on the CEM data obtained from each experimental run. In this case, the table contained the CEM data, in which each row contained 30 second readings and the columns were combustion parameters. The data were *UV*-scaled and the MSPC indicated when the process had reached steady state. It also indicated specific trends or transient discontinuities in the combustion process. The MSPC output of this study was displayed in Shewhart control charts, which calculated a rolling average of all the CEM data in one variable and caclulated upper and lower control limits (2 and 3 times the standard deviation). A value outside the control limit implied that the combustion process had been disturbed. The parameter that caused the disturbance could then be localized using the S*core contribution plot*. Since this was a line plot, PC1 could be used.

4. Results and Discussion

Results from the 23 experimental runs with combustion data and data from analyses of the 78 dioxin samples are summarized below. The data for each individual run are presented in Tables 14-19 of Appendix 1.

4.1 Baseline runs

In the first run (baseline run 1), two periods of increased CO concentration (800 and 200 ppm peaks) occurred early in the experiment. At the time this was not considered to be problematic. However, evaluation of all the data indicated that these were the only such occurrences. Data from this run were therefore excluded from calculations of the baseline run averages. The data in Table 8 demonstrate that the target values for the chosen combustion parameters were reached. The average concentrations and coefficient of variance (CV) for the combustion gases measured in the baseline runs are shown in Table 9. Very low concentrations were observed for SO_2, NH_3 and CH_4. The low SO_2 level was probably due to the low sulphur content of the fuel, while the low NH_3 and CH_4 values were probably due to efficient combustion and sufficient O_2 concentrations.

Table 8. Average values of target combustion parameters during sampling in baseline runs 2-5

Combustion parameter	Value	Residence time [seconds]
Bed [°C]	820	
Freeboard[a] [°C]	800	5.1[c]
P2[b] [°C]	640	0.1[d]
P3[b] [°C]	395	1.4[d]
P4[b] [°C]	295	2.3[d]
P7[b] [°C]	210	4.4[d]
H_2O [vol%]	8	
O_2 [vol% dg]	11	
Excess air ratio (λ)	2.1	
CO [ppm dg]	<3	
Fuel load [kg/hour]	0.9	
Fuel load [kW]	4.9	
PM[c] [mg/Nm^3 dg 11% O_2]	1200	

[a] Freeboard temperature at T4 and T5.

[b] Temperature at the sampling port in the convector section.

[c] Accumulated residence time in freeboard.

[d] Residence time in post-combustion zone.

Table 9. Average concentrations and coefficient of variasnce (CV) of combustion gases during sampling in baseline runs 2-5 (dry gas).

	H_2O	CO_2	SO_2	NO_2	CO	NO	HCl	NH_3	N_2O	CH_4	O_2
	vol%	vol%	ppm	ppm	ppm	ppm	ppm	ppm	ppm	ppm	vol%
Average	7.8	9.0	<0.5	32	3	460	209	<0.5	49	<0.5	11
CV [%]	6	9	-	5	11	10	15	-	5	-	5

No major increases or decreases were observed in PCDD, PCDF, I-TEQ or Sum PCB concentrations when the gas temperature fell from 400 to 200 °C during passage through the post-combustion zone (Figures 11 and 12). However, planar PCB and HCB concentrations increased with reductions in temperature and increases in residence time in the post-combustion zone (Figure 12). The data imply that formation was highest at around 400 °C. The CVs for the I-TEQ, PCDD, PCDF, and HCB data acquired at each sampling point were all < 30%. However, the CVs for the PCB and planar-PCB data acquired at the P4/300 °C and P7/200 °C sampling point/temperatures were higher (up to 60%), indicating that rates of PCB formation were highly variable. Results from sampling point P2 are discussed in section *4.2 High temperature formation – gas-phase formation*.

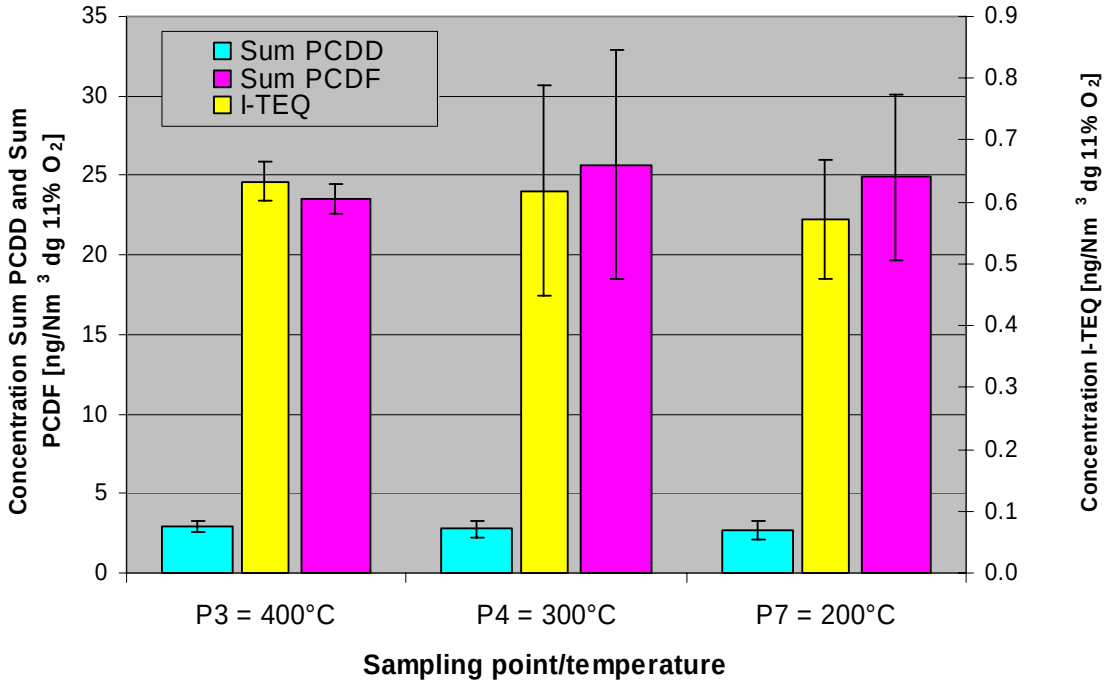

Figure 11. Average I-TEQ, PCDD and PCDF concentrations in baseline runs 2-5. The error bars represent ± 1 standard deviations.

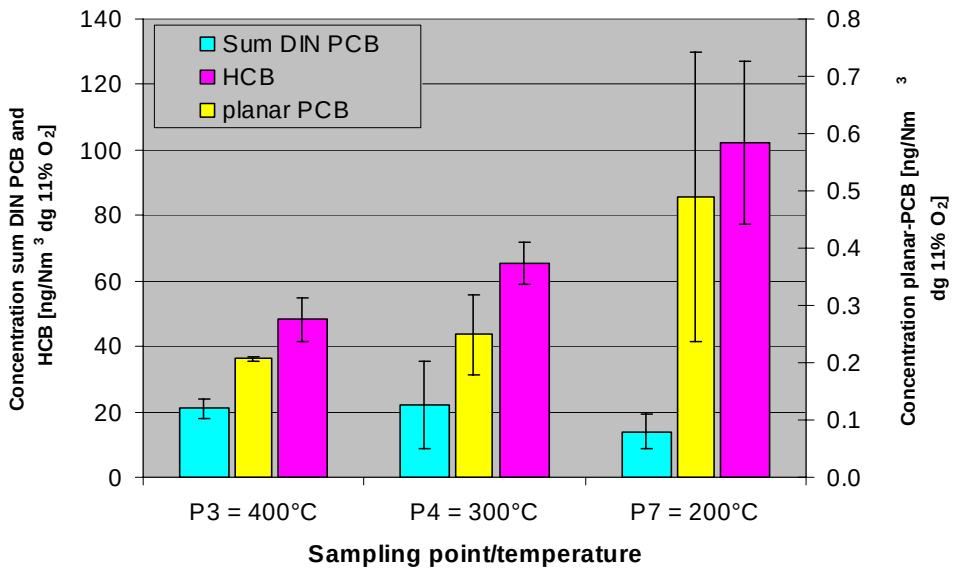

Figure 12. Average concentrations of PCBs (sum DIN-PCB and planar PCB) and HCB in baseline runs 2-5. The error bars represent ± 1 standard deviations.

4.2 High temperature formation – gas-phase formation

In the first experimental campaign sampling was performed at sampling points P2, P3 and P7. The results from sampling point P2 are discussed in this section. The temperature at this point was around 640 °C, except in runs 13 and 14 with modified freeboard temperatures. Temperatures at P2 for runs 13 and 14 were 730 °C and 545 °C, respectively. The I-TEQ concentrations at 640 °C and 545 °C were > 20 times lower than at 200 °C (Table 10). However, the I-TEQ and PCDD concentrations at 730 °C were respectively 12 and 50 times greater than at 640 °C. This could be due to a sample defect or because quenching in the cooled probe was not rapid enough. To verify the results for the 640°C samples, the cooled probe was modified as described in section *3.4 Sampling*. The result from run 10 (640 °C), using the modified cooled probe, was below the detection limit. This differ with results from earlier studies on high temperature formation (gas-phase formation) performed at Umeå University.

Table 10. Results of high temperature experimental runs.

Concentration [ng/Nm^3 dg 11% O_2]	**P2 = 640 °C Average[a]**	**P2 = 730 °C Run 13:1**	**P2 = 545 °C Run 14:1**	**P2 = 640 °C Run 10:1**	**P7 = 200 °C Average[a]**
I-TEQ	0.03	0.37	0.05	<0.01[b]	0.77
PCDF	0.6	10	1.3	<0.1[b]	30
PCDD	1.7	40	1.2	<0.1[b]	3.2

[a] Average value of runs 2 and 3.

[b] Not detected.

4.3 Residence times and temperatures in the post-combustion zone

The I-TEQ concentrations in samples from the four investigated temperature-residence time profiles are presented in Figure 13. The baseline temperature-residence time profile is discussed above. The I-TEQ concentrations in samples from sampling point/temperature P7 (260 °C) in the high temperature-residence time profile runs (6-8) decreased in successive runs. This is discussed further in section *4.7.2* M*emory effects in the post-combustion zone*. Since the samples from runs 6 and 7 taken at P7 (260 °C) were compromised by memory effects they were excluded from the discussion of residence times. Nevertheless, the data from runs 6-8 showed that I-TEQ concentrations increased with increases in residence time and reductions in temperature in the post-combustion zone (Figure 13). However, the I-TEQ concentrations were lower than those found in the baseline runs. The residence time at 400 °C was very short - 0.7 seconds between 400 and 360 °C, in convector section 3 (Figure 14). In contrast, in the baseline runs and runs 11-12 there was a residence time of 0.7 seconds at 400 °C in convector section 2.

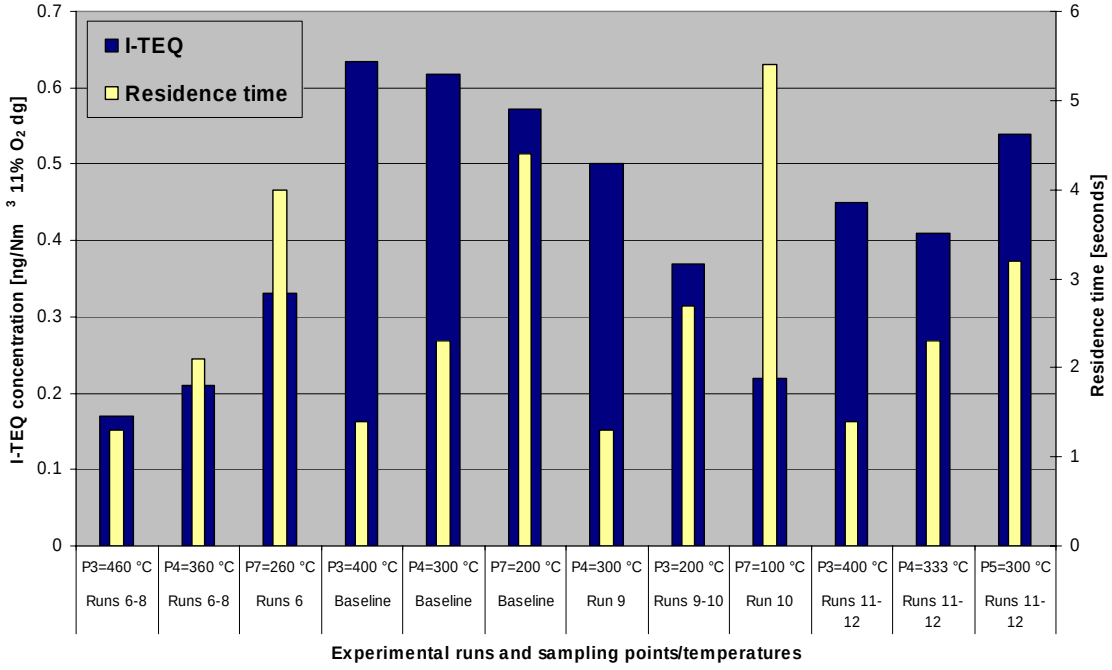

Figure 13. I-TEQ concentrations in the flue gas observed for each of the temperature-residence time profiles of the post-combustion zone.

In the low temperature-residence time profile runs (9 and 10) the I-TEQ concentrations at sample point/temperature P3 (300 °C) were similar to those found in the baseline runs (within the CV). For these runs the residence time between 400 and 300 °C was 0.9 seconds in convector section 2.

The results imply that dioxin formation was highest at 400 °C or 300 °C, at residence times of 0.7 seconds or 0.9 seconds, respectively, in the 2nd convector section,

suggesting that the conditions in convector section 2 were different from those in the other sections. Possible reasons for this could include: differences in particle amounts or sizes; slower cooling allowing equilibrium to be approached for oxidation/sulphation of inorganic constituents; and/or the bends of the convector section causing the particles and the gas stream to separate, and the first bend being passed before the threshold temperature was reached in runs 6-8. A residence time of 1.6 seconds (0.7+0.9 seconds) at 400-300 °C under the same conditions as in convector 2 would result in a higher I-TEQ concentration (about 1 ng/Nm^3 in this case). Further increases in residence time and temperature would lead to additional formation. This is in accordance with the optimum formation conditions for dioxins. However, the effects of variations in particle amount, particle size and elemental distribution on dioxin formation at different temperatures and residence times require further investigation.

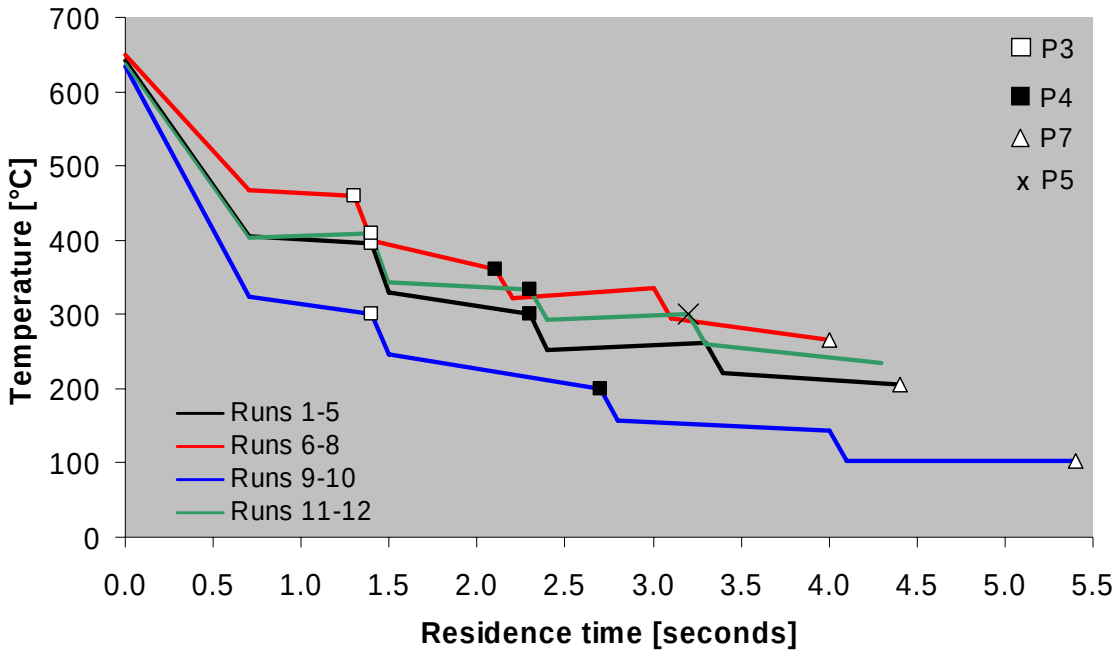

Figure 14. Temperature-residence time profiles investigated in the post-combustion zone. Sharp drops are due to heat losses at the ends of the convector tubes (no outside heating).

4.4 Freeboard temperatures

In experimental runs 13 and 14 the freeboard temperature was increased or decreased relative to the baseline runs. Increasing the freeboard temperatures (T4 and T5) from 800 °C to 950 °C did not significantly affect the I-TEQ concentrations of the flue gas in the post-combustion zone, compared to the baseline concentrations (Figure 15). The Sum DIN PCB, planar-PCB and HCB concentrations in the flue gas of the post-combustion zone did not significantly change either (Figure 16). The residence time in the freeboard was about 5 seconds at a temperature of 800 °C and about 4.5 seconds at 950 °C. These residence times are quite long compared to the 2 seconds recommended in the literature

and may explain why no change was detected in the I-TEQ concentrations in flue gas of the post-combustion zone.

In experimental run 14 the freeboard temperatures (T4 and T5) were decreased to 655 °C compared to 800 °C in baseline runs. The I-TEQ concentrations in the flue gas in the post-combustion zone were double the baseline concentrations (Figure 15). Similar increases were observed in the planar-PCBs, but no major effect was observed on the sum DIN PCB and HCB concentrations. The increase in I-TEQ concentrations was probably due to incomplete combustion because of the low secondary-combustion zone temperature. The CO concentration in the flue gas increased from about 3 ppm in the baseline runs to 40 ppm. The CO concentration was steady for the entire run, *i.e.* no CO peaks.

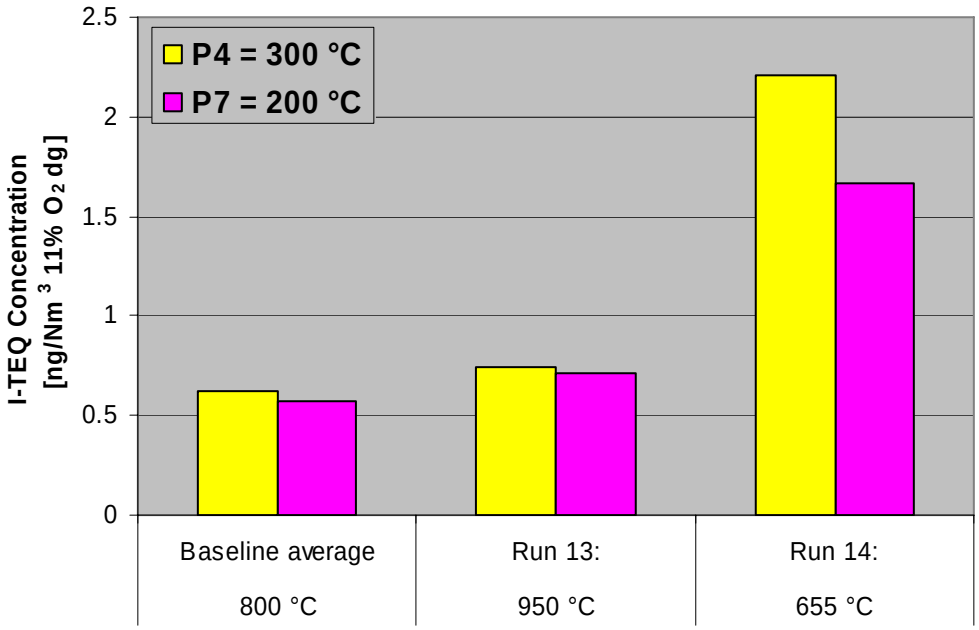

Figure 15. I-TEQ concentrations for runs with freeboard temperatures of 655, 800 and 950 °C, sampled at 300 and 200 °C in the post-combustion zone.

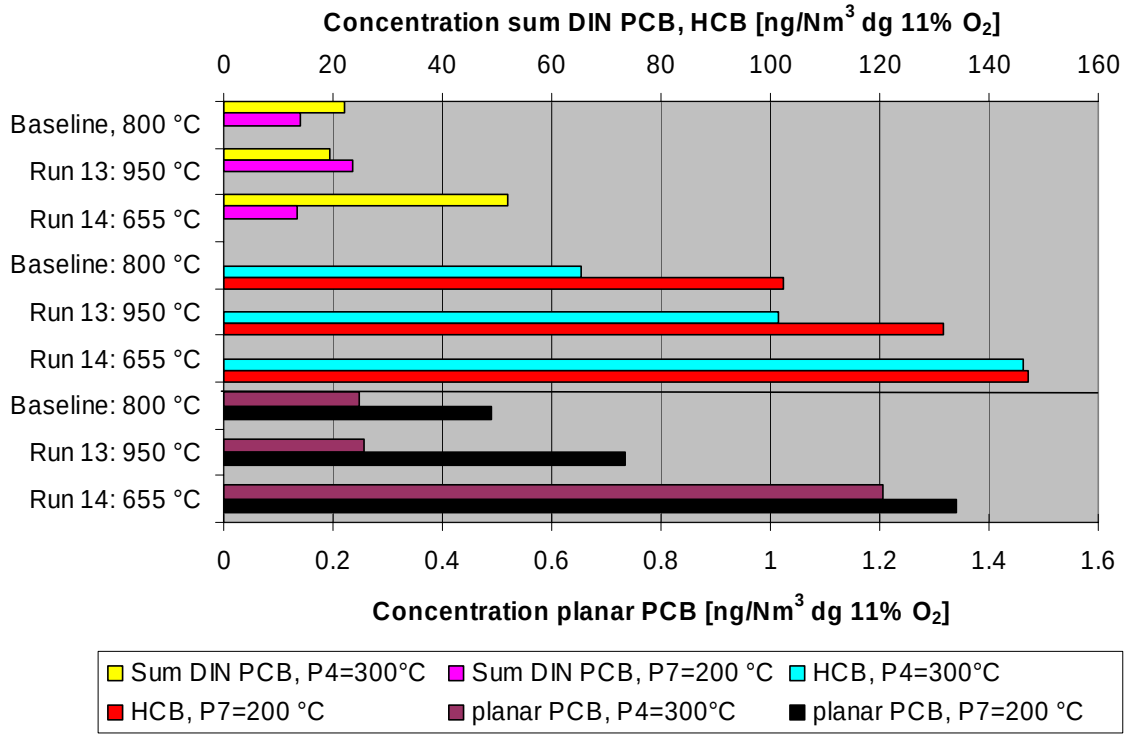

Figure 16. PCB and HCB concentrations for runs with freeboard temperatures 655, 800 and 950 °C, sampled at 300 and 200 °C in the post-combustion zone.

4.5 Reduced fuel load

In experimental runs 15 and 16 the fuel load **(0.6 kg/h)** was reduced compared to the load used in the baseline runs (0.9 kg/h), resulting in a longer residence time in the post-combustion zone (Figure 17) and freeboard due to the decreased air supply; the freeboard residence time was 7.4 seconds compared to 5.1 seconds in baseline runs. Differences in results (Figures 18 and 19) were observed for runs 15 and 16. In run 15 the dioxin, planar PCB and HCB concentrations in the flue gas sampled at 200 °C were much greater than in baseline runs. These high concentrations were probably due to memory effects in the post-combustion zone, which are discussed in section *4.7.2 Memory effects in the post-combustion zone*. In run 16 (with a reduced fuel load) there were lower dioxin, planar PCB and HCB concentrations than in baseline runs. The sum DIN PCB concentration in the flue gas showed no significant change.

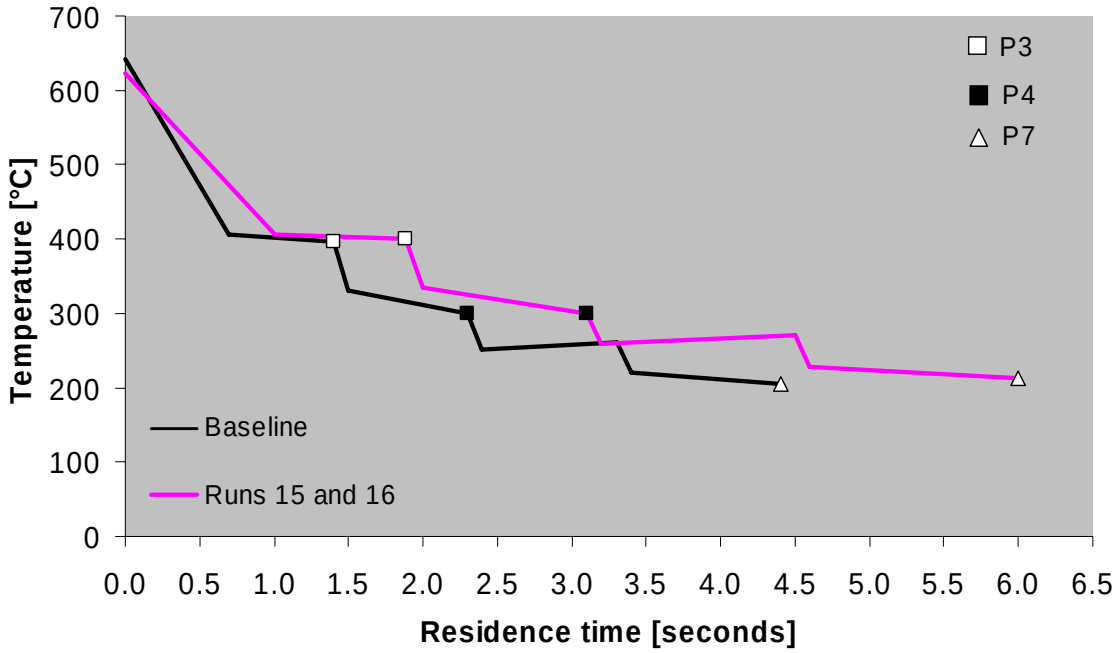

Figure 17. Temperature-residence time profiles in the post-combustion zone in baseline and runs 15 and 16 (reduced fuel load). The sharp drops are due to heat losses at the ends of the convector tubes (no outside heating).

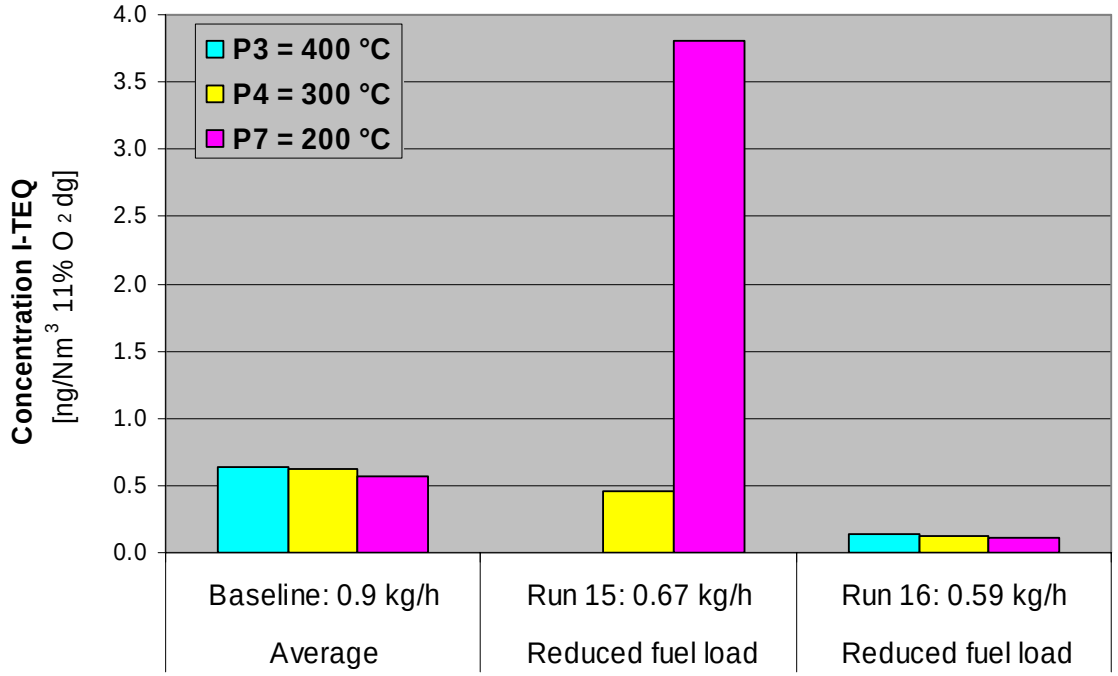

Figure 18. I-TEQ concentrations for experimental runs 15 and 16 with reduced fuel load, ca. 0.6 kg/h, sampled at P3 (400 °C), P4 (300 °C) and P7 (200 °C) in the post-combustion zone.

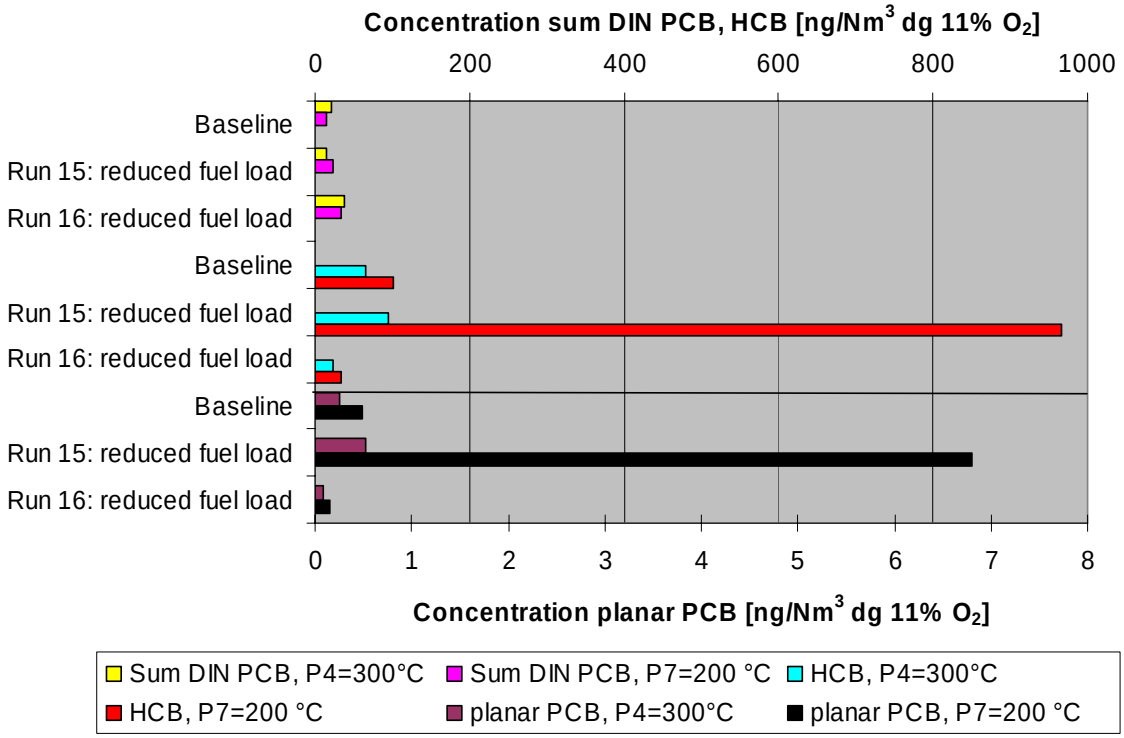

Figure 19. PCB and HCB concentrations for experimental runs 15 and 16 with reduced fuel load, ca. 0.6 kg/h, sampled at P4 (300 °C) and P7 (200 °C) in the post-combustion zone. Results from sampling at P3 (400 °C) are shown in Table 14, Appendix 1.

4.6 Fuel and additives

Experimental runs 17-21 included variations in the Cl, H_2O, Cu and SO_2 concentrations in the fuel, which affected flue gas composition (Table 11).

Increasing the chlorine content (run 17) led to a ca. 2.5-fold increase in the HCl level in the flue gas compared to the baseline level, which significantly influenced the I-TEQ, HCB and planar PCB concentrations in the flue gas in the post-combustion zone (Figures 20 and 21). In addition, I-TEQ concentrations increased to about 10 times the baseline concentrations. These results agreed well with earlier studies by Wikström et al. (*16*). No significant changes were observed in the sum DIN PCB concentration from baseline.

Table. 11. CEM data for constituents of flue gas from incineration of MSW with added Cl, H_2O, Cu and S.

Run	Experiment	H_2O	CO_2	SO_2	NO_2	CO	NO	HCl	NH_3	N_2O	CH_4	O_2
		Vol %	Vol %	ppm	ppm	ppm	ppm	ppm	ppm	ppm	ppm	Vol %
1	Baseline	7.8	9.0	<0.5	32	3	460	209	<0.5	49	<0.5	11
17	Increased Cl-level in the fuel	7.6	9.2	<0.5	32	3	502	538	0.6	53	<0.5	11
18	Increased Cu-level in the fuel	8.0	9.5	<0.5	38	4	607	187	<0.5	36	<0.5	11
19	Addition of SO_2 (1.9% S)	7.6	9.0	131	12	3	409	319	<0.5	77	<0.5	11
20	Addition of SO_2 (3.9% S)	7.7	9.3	572	10	4	405	366	1.4	76	2.6	10
21	Addition of H_2O	21	10.0	<0.5	27	3	476	236	0.8	75	<0.5	11

Increasing the fuel's copper content (run 18) resulted in an increased concentration of NO in the flue gas compared to the baseline level. An increase in NO usually requires an increase in oxygen; however, the O_2 level was similar to the baseline level. The I-TEQ concentrations in the flue gas in the post combustion zone were reduced (Figure 20). These results agree on the theory on the coppers catalytically effect on oxidation proposed in the literature. Whether or not this is the cause here, can not be stressed by this experiment. No deviations from baseline levels were observed for concentrations of DIN-PCBs, planar PCBs and HCB (Figure 21).

In experimental run 21 water was added to the combustion zone, resulting in a concentration of 21 vol% H_2O in the flue gas, compared to the baseline value of 7.8 vol%. At P3 (300 °C) the I-TEQ concentration was lower than the baseline value and at P7 (200 °C) the I-TEQ concentration was greater than the baseline value (Figure 20). This suggests reasons for findings of both increases and decreases of PCDD/F levels in previous studies following water addition. The planar PCB and HCB concentrations in the flue gas at the sampling points/temperatures followed the trend of the I-TEQ levels, while the sum of DIN-PCBs was unaffected (Figure 21). However, data from runs 18 and 21 were at the margins of the spread of results.

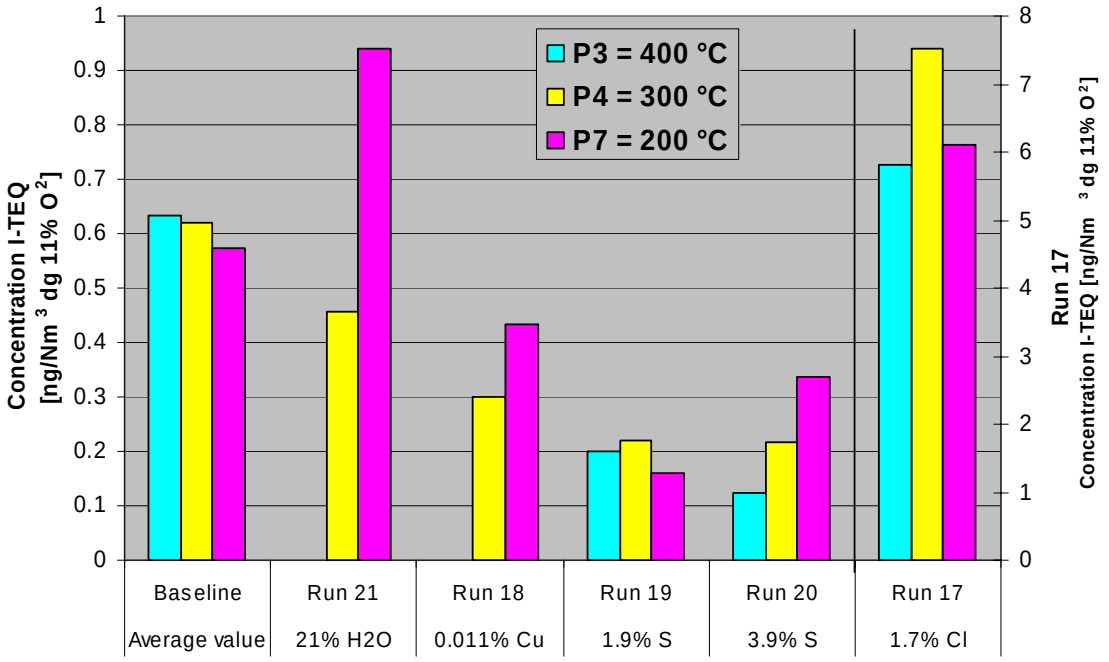

Figure 20. Dioxin I-TEQ concentrations in runs with additions of H_2O, Cu, S and Cl at sampling points/temperatures P3 (400 °C), P4 (300 °C) and P7 (200 °C) in the post-combustion zone.

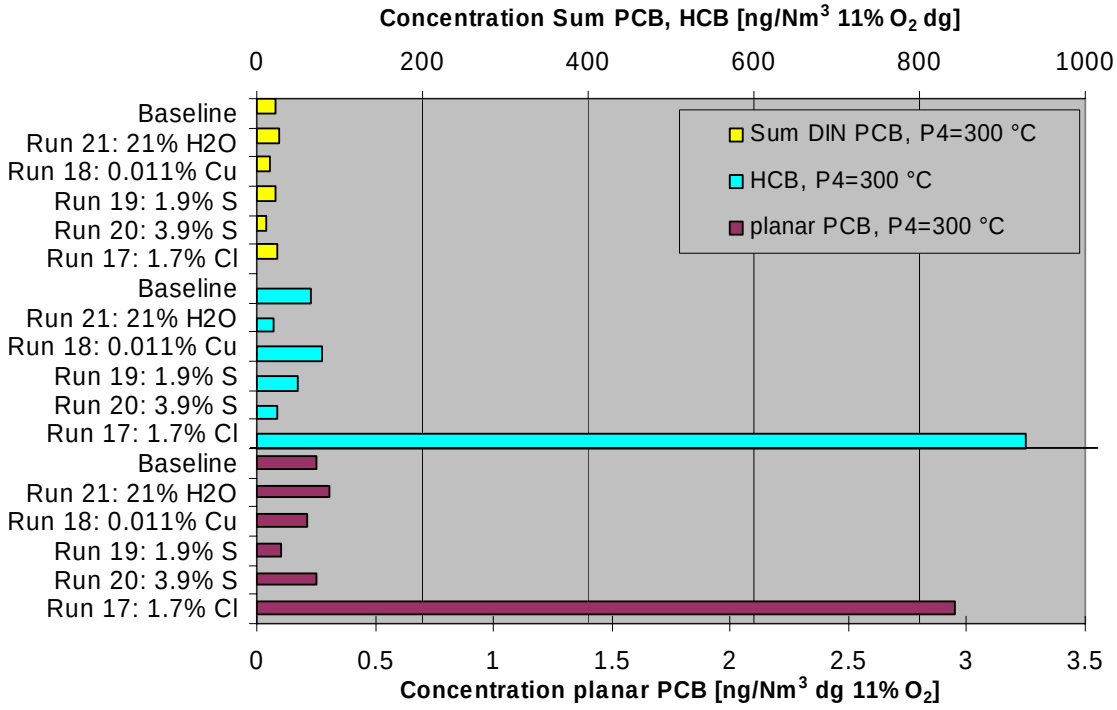

Figure 21. PCB and HCB concentrations in runs with additions of H_2O, Cu, S and Cl at sampling point P4 (300 °C) in the post-combustion zone. Results sampled at P3 (400 °C) and P7 (200 °C) are shown in Table 14, Appendix 1.

Addition of SO_2 in the combustion zone significantly altered the composition of the flue gases, increasing SO_2, HCl, and N_2O levels and decreasing NO_2 and NO levels compared to baseline levels (Table 11). The SO_2 in the flue gas increased from < 0.5 ppm to 130 and 570 ppm in runs 19 (1.9% S) and 20 (3.9% S), respectively, resulting in S:Cl ratios of 0.4 and 1.6 (by mass) in runs 19 and 20 (Table 12). The I-TEQ concentration in the flue gas in the post-combustion zone decreased by about 70% in both runs, except at sampling point/temperature P7 (200 °C) in run 20 (3.9% S) (Figure 20). The CEM data showed an increase of CH_4 content from < 0.5 ppm to 2.6 ppm in run 20 (3.9% S). In this run there was a tendency for the I-TEQ concentration in the flue gas to increase with reductions in temperature in the post-combustion zone, which agrees with earlier studies in the literature. In run 19 (1.9% S) the planar PCB concentration in the flue gas decreased by about 50% compared to the baseline. No significant effect was observed on the HCB concentration. In run 20 (3.9% S) the planar PCB and HCB concentrations in the flue gas, increased. No significant change was evident in the DIN-PCB concentrations in either experiment.

Table 12. Sulphur and S:Cl ratio in the fuel and the flue gas.

	Baseline	Run 19	Run 20
S in the fuel [%]	0.07	1.9[b]	3.9[b]
S:Cl in the fuel [by mass]	0.1	2.7[b]	5.6[b]
S:Cl in the fuel [by molar mass]	0.1	3.0[b]	6.2[b]
SO_2[a] [ppm]	<0.5	130	570
S:Cl[a] (SO_2:HCl) [by mass]	-	0.4	1.6
S:Cl[a] [by molar mass]	-	1.6	3.1

[a] In the flue gas.

[b] Sulphur content calculated from the concentration added and the fuel feed rate.

4.7 Transient combustion conditions and memory effects

4.7.1 Transient combustion conditions with following memory effects

Transient conditions and following memory effects were evaluated in an extended experiment (run 3). CO levels were observed to return to their initial values immediately after the peaks indicating transient periods (Figure 22). A substantial increase I-TEQ concentration was observed during the transient disruption (Figure 23). Memory effects in the post-combustion zone declined as time increased after the disturbance, as noted by other researchers. Memory effects were greater at lower temperatures in the post-combustion zone (*i.e.* sampling point/temperature 200 °C). The DIN-PCB, planar PCB and HCB concentrations in the flue gas followed the same trend (Figure 24).

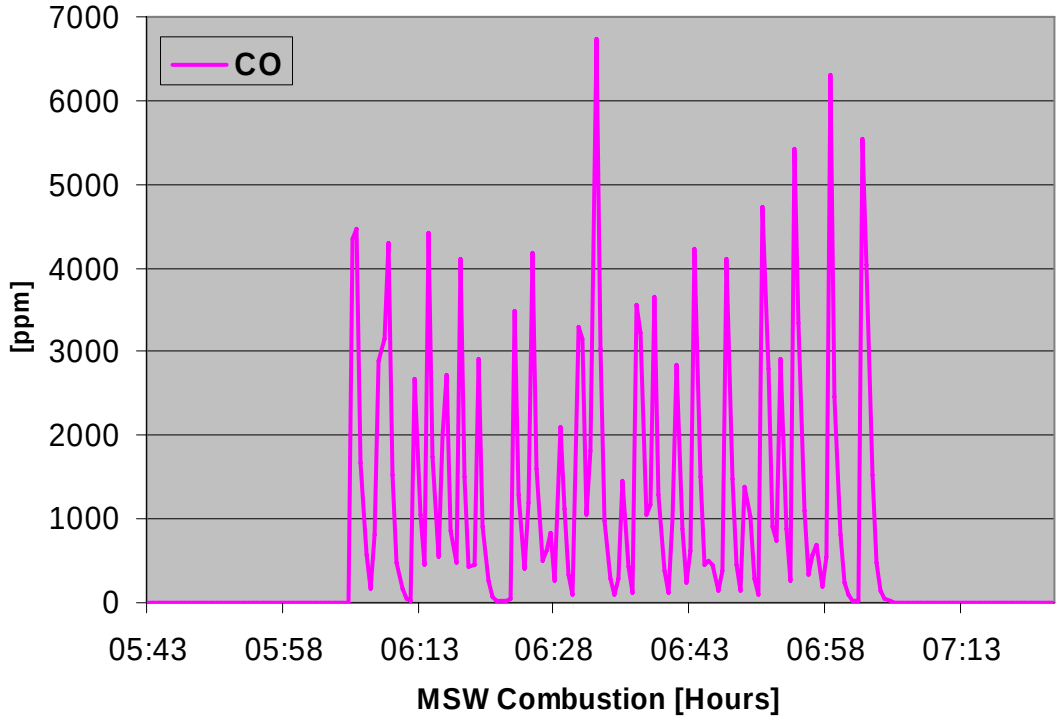

Figure 22. CEM data from the transient combustion period, illustrating the variation in CO concentration.

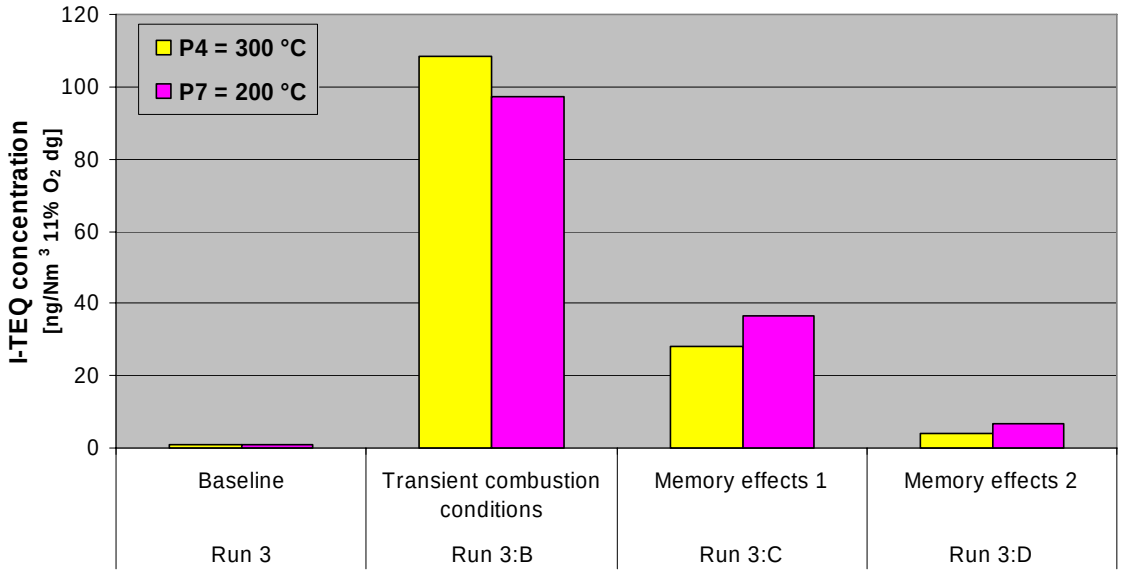

Figure 23. Dioxin I-TEQ concentrations in the flue gas in the post-combustion zone during MSW incineration before, during and after a transient combustion period.

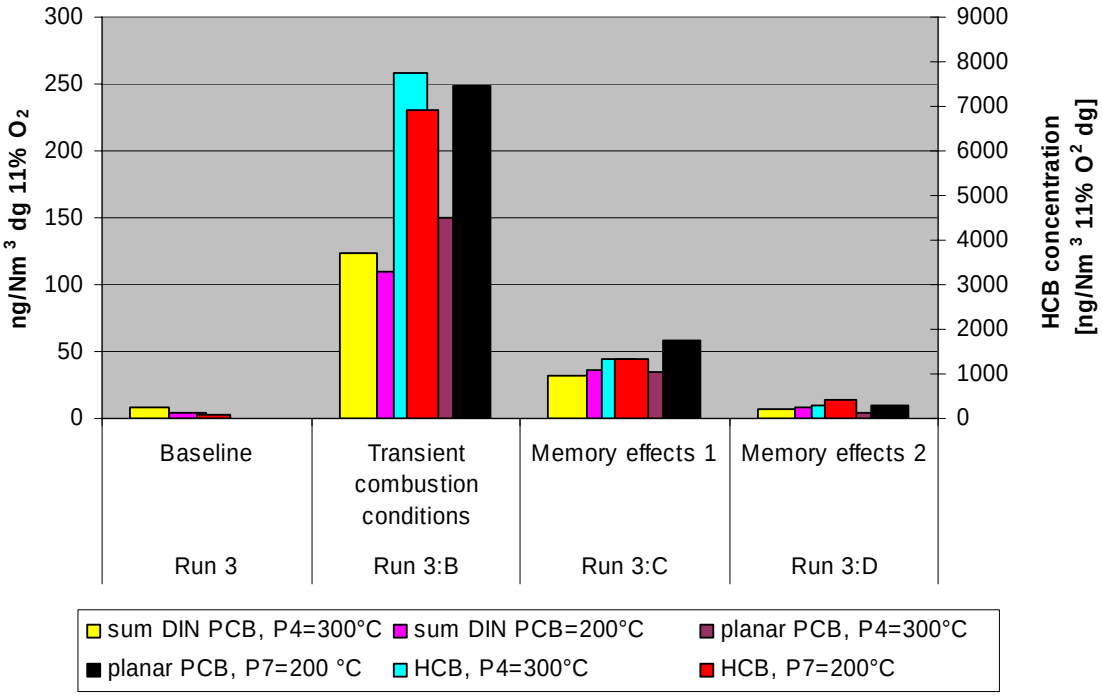

Figure 24. PCB and HCB concentrations in the flue gas in the post-combustion zone during MSW incineration before, during and after a transient combustion period.

To investigate the formation of PCDD/Fs during and after transient combustion conditions, the congener profiles of the TeCDD homologue group in samples obtained during these times were studied by inspecting GC-HRMS chromatograms. The results revealed significant differences in the congener patterns. During transient disturbances, greater increases were found for congeners 1,3,6,8- and 1,3,7,9-TeCDD than for the other TeCDD congeners (Figure 25). In the period when memory effects were exerting their influence, the proportions of 1,3,6,8- and 1,3,7,9-TeCDD decreased in comparison to those in the transient combustion sample. Recently these congeners have been reported to increase during and after transient conditions in full-scale plants (*35*,*38*).

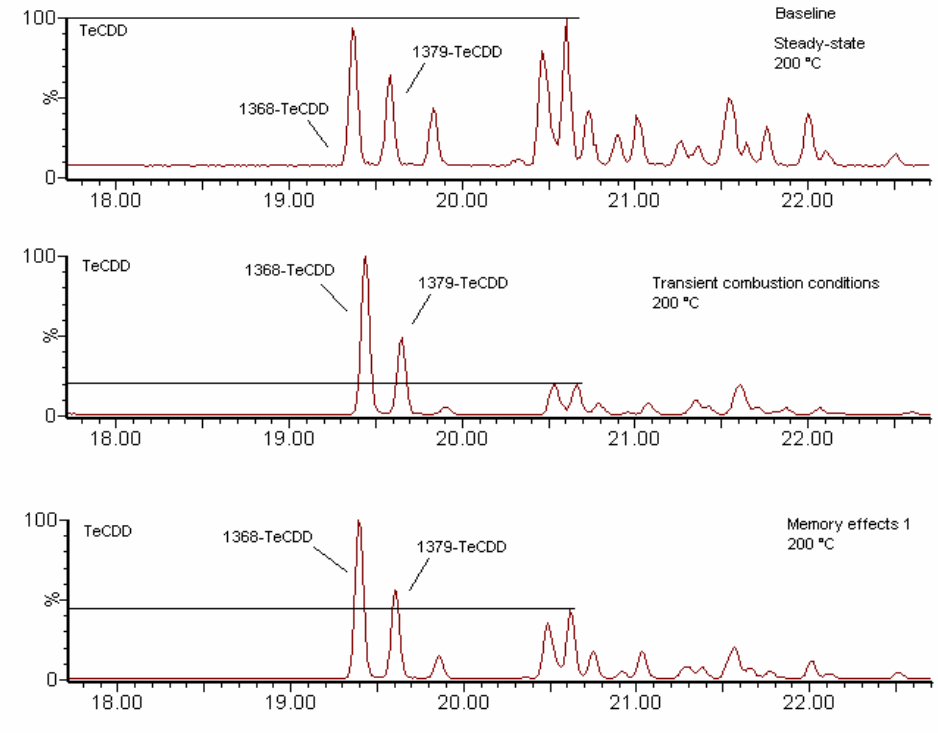

Figure 25. GC-HRMS chromatograms of tetra-chlorinated dibenzo-*p*-dioxins found in baseline runs (steady-state), under transient conditions and in periods with memory effects due to transient conditions. The y-axis shows the relative abundance on a peak height basis.

4.7.2 Reduced O_2 levels in the flue gas

In runs 22 and 23, the O_2 level was reduced in the flue gas, resulting in increased CO concentrations because of incomplete combustion (Table 13). The I-TEQ concentration in the flue gas increased significantly (Figure 26), but was not directly correlated to the CO concentration in the flue gas. The I-TEQ content of flue gas from run 23 (2.4% O_2) was half that of run 22 (3.4% O_2). The CO concentration prior to the sampling period could have affected these results. The CEM data showed there was a lower average CO concentration in run 23 (2.4% O_2) than in run 22 (3.4% O_2) (Table 13). The CO peaks also appeared to be irregular, as illustrated in Figure 27, suggesting that memory effects also influenced the results of these two runs. The findings from run 3 (above) imply that transient conditions (with a CO peak) increase dioxin formation and the formation rate decreases with time after the disturbance.

Transient combustion conditions (run 3B) generated much higher I-TEQ concentrations than runs 22 and 23. This could be due to higher O_2 levels, but could also be influenced by the regularity of transient conditions. For runs 22 and 23 the planar PCB and HCB concentrations in the flue gas followed the same pattern as the I-TEQ (Figure 28). The DIN-PCB concentration showed no significant change between runs 22 and 23.

Table 13. Dioxin concentrations in experimental runs with reduced O_2 and increased CO levels, sampling point/temperature P4/300 °C.

Run	I-TEQ [ng/Nm^3] not normalized to 11% O_2	I-TEQ [ng/Nm^3 11% O_2 dg]	O_2 (%)	CO during sampling (ppm)	CO before sampling (ppm)
Baseline	0.6	0.6	11	<3	<3
3:B	133	109	8.8	1577	<3
22	7.5	4.3	3.4	550	566
23	4.1	2.2	2.4	1254	431

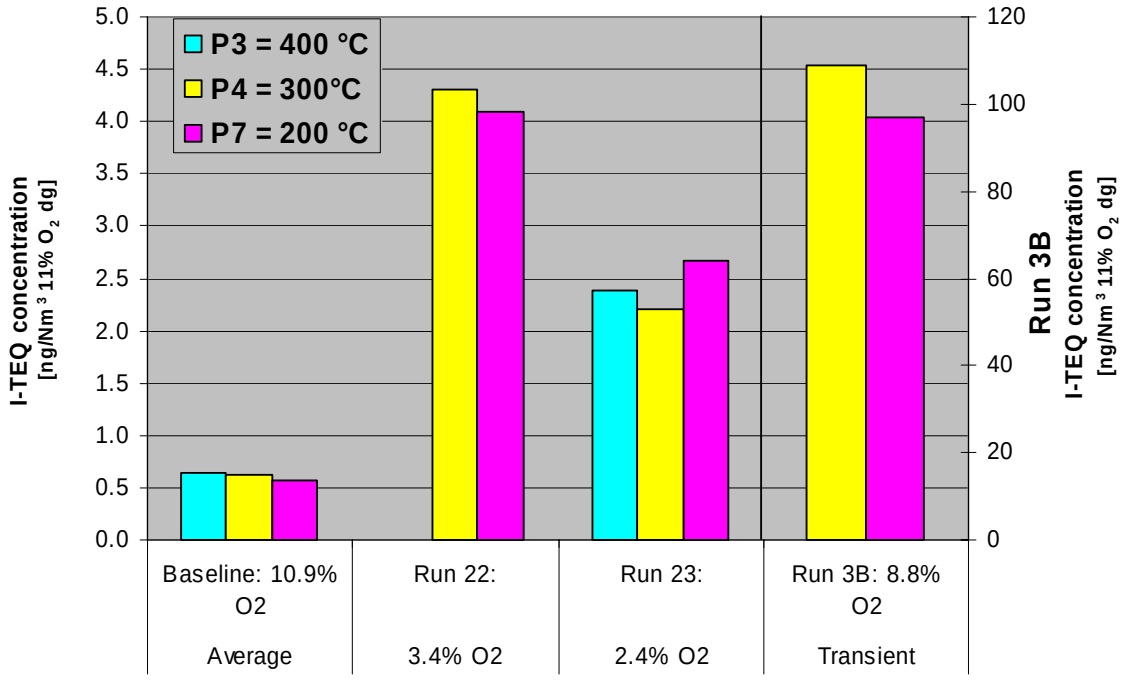

Figure 26. Dioxin (I-TEQ) concentrations for runs with reduced O_2 level and increased CO level compared to baseline.

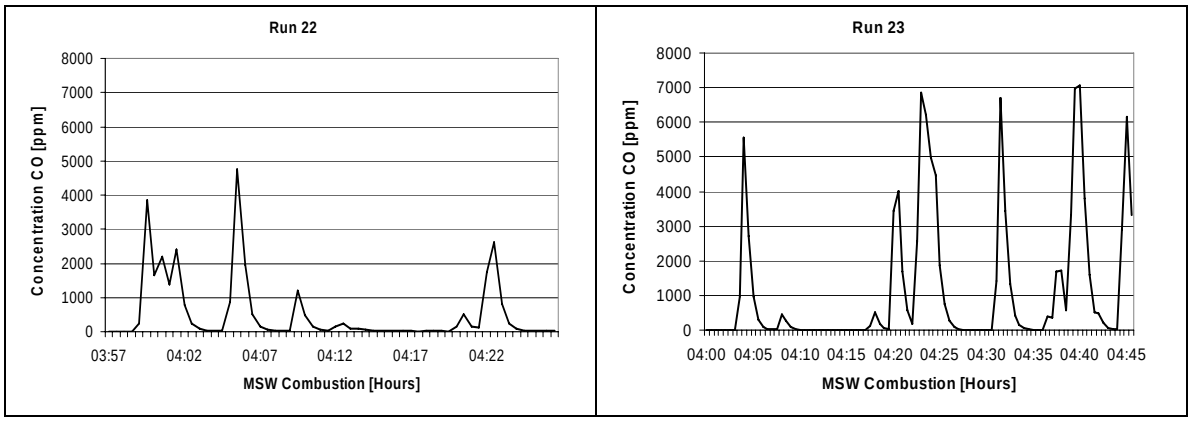

Figure 27. CEM data showing irregular increases in CO concentrations in the flue gas, runs 22 and 23.

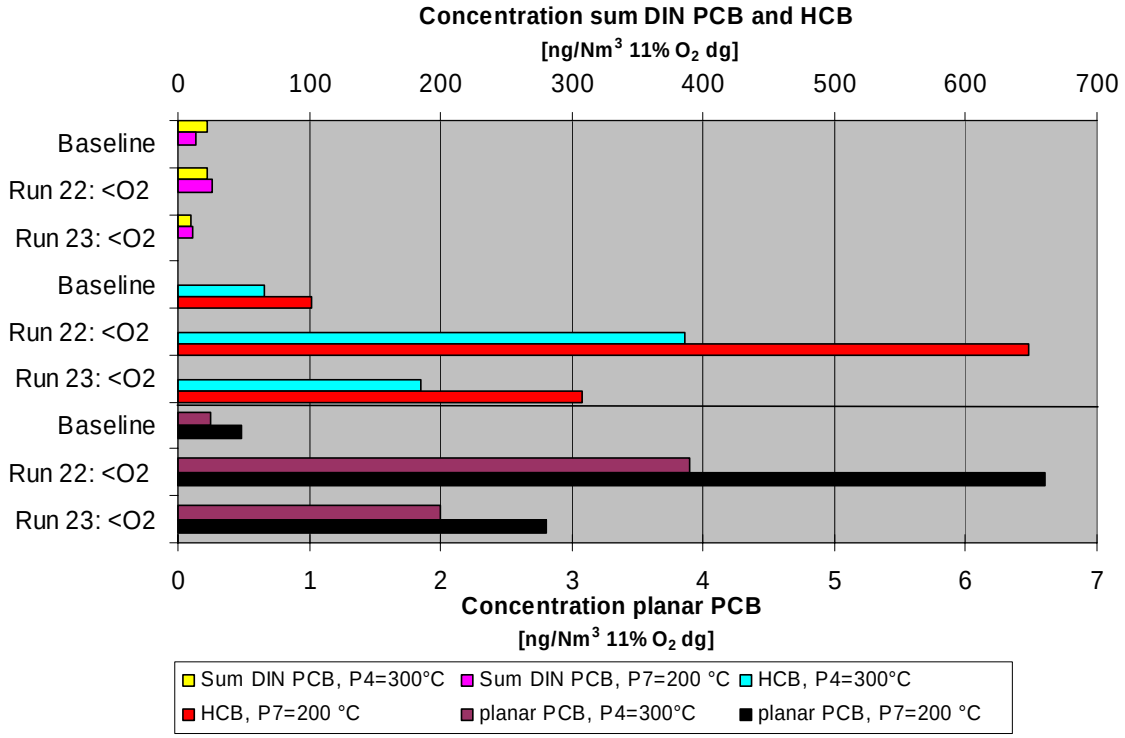

Figure 28. PCB and HCB concentrations for runs with reduced O_2 level**s** and increased CO levels compared to baseline.

4.7.3 Memory effects in the post combustion zone

In two experiments the triplicate or replicate runs showed a clear trend or a substantial deviation from each other. The first indication of deviations between runs was in runs 6-7 (high temperature in the convector), as shown in Figure 29. In these runs I-TEQ concentrations in the flue gas at sampling point/temperature P7/ 260 °C with declined with successive replicates. As in run 3 with the transient combustion conditions, the congener profile of the TeCDD homologue group was studied. The results were similar to

those shown for transient combustion conditions and memory effects, *i.e* higher levels of 1,3,6,8- and 1,3,7,9-TeCDD than of the other TeCDD congeners (Figure 35, Appendix 2). These patterns can be compared to the baseline pattern in Figure 25.

The second deviation between runs was in runs 15 and 16, shown in Figure 18 (reduced fuel, see section *4.5 Reduced fuel load*). Analyses of the congener profiles of the TeCDD homologue group obtained in samples from these runs showed that in run 15 the congeners 1,3,6,8- and 1,3,7,9-TeCDD dominated the TeCDD congener profile (Figure 36, Appendix 3).

These findings indicate that the increases in the dioxin concentration were probably due to memory effects which are *de novo* based *i.e.* the dioxins were formed from chlorides and carbon structures deposited on the convector walls. The results are of interest since they show large increases in dioxin concentrations even though the system was thoroughly cleaned. This indicates that very small particles are important in the formation of dioxins.

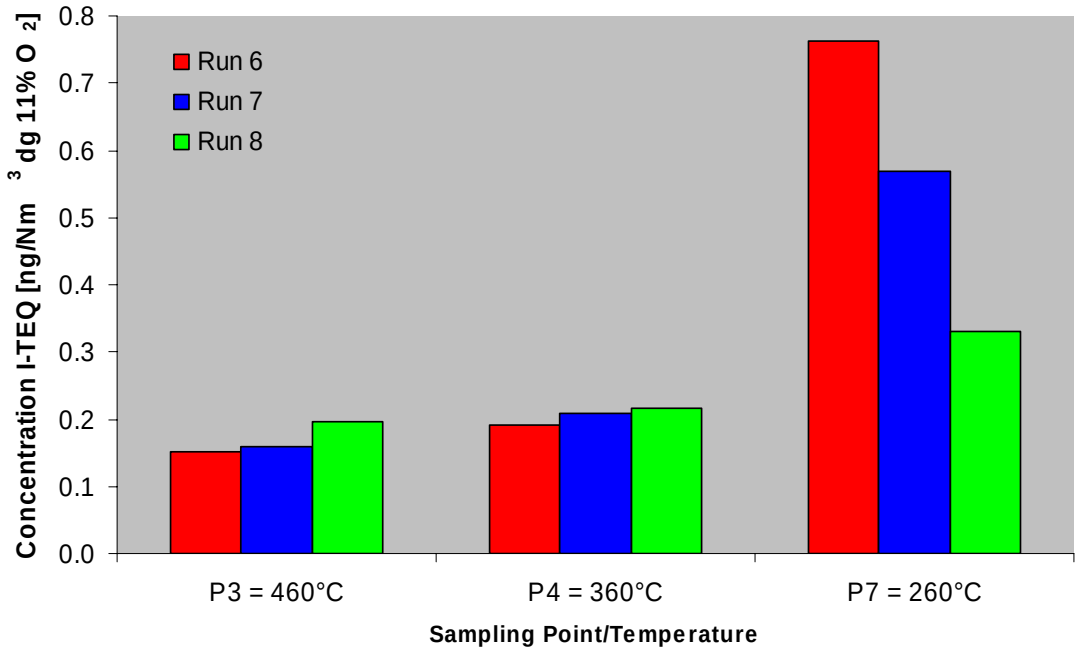

Figure 29. Dioxin (I-TEQ) concentrations in samples obtained from runs 6-7 (temperature profile 460-260 °C).

4.8 Overview of the results

Figure 30 provides an overview of the experiments and displays dioxin concentrations from sampling at 300 °C in the post-combustion zone. A comparison between runs shows that a reduced fuel load or an increase in sulphur content reduces dioxin formation, whereas an increase in the chlorine level in the fuel, a temperature of 660 °C in the

freeboard or transient combustion conditions (incomplete combustion) increases dioxin formation.

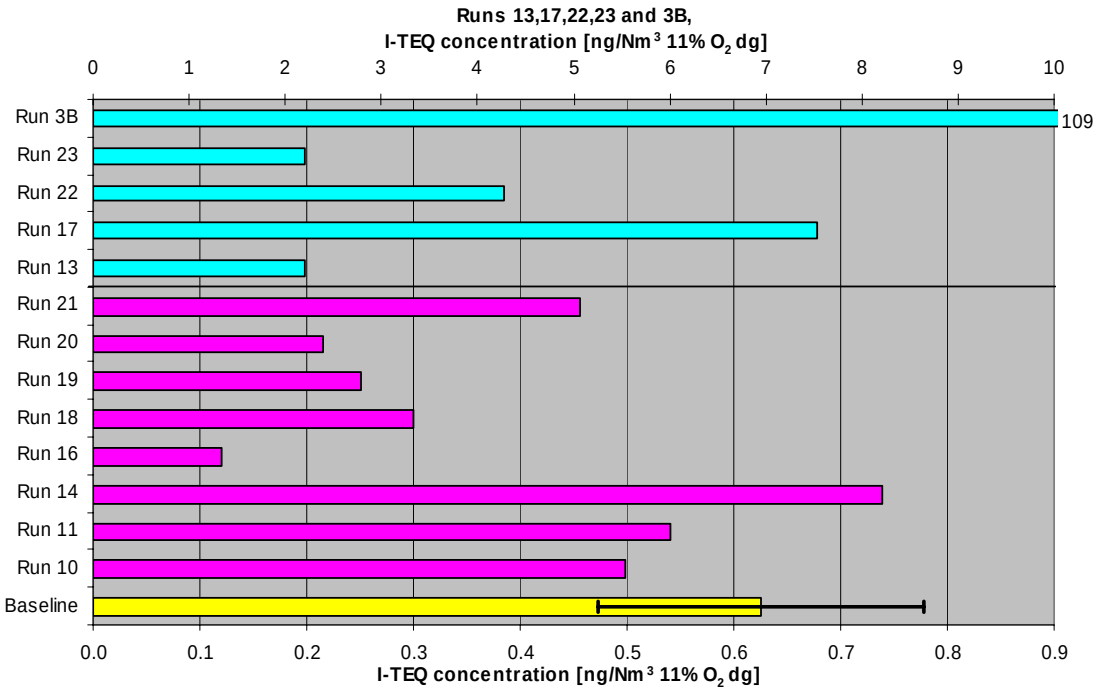

Run	Experiment	Run	Experiment
10	Low temperature in the convector	19	Addition of SO_2 1.9% in the fuel
11	Temperature changes in the convector	20	Addition of SO_2 3.9%
13	Reduced temperature in the freeboard 660°C	21	Addition of H_2O
14	Increased temperature in the freeboard 950°C	22	Reduced O_2-level in the flue gas
16	Reduced fuel load	23	Reduced O_2-level in the flue gas
17	Increased Cl-level in the fuel	3B	Transient conditions
18	Increased Cu-level in the fuel		

Figure 30. Results from 13 experiments. Dioxin (I-TEQ) concentrations obtained from runs sampled at 300 °C in the post-combustion zone.

4.9 Statistical evaluation

4.9.1 Multivariate statistical process control - MSPC

MSPC analysis of the experimental data showed that the combustion conditions were stable. It also showed that steady state, according to the CEM data, was established after about 2 hours of MSW combustion (Figure 31). MSPC detected a disturbance in run 20 (3.9% S in the fuel) after about 3.5 hours of MSW combustion (Figure 32). This disturbance was evaluated further using a score contribution plot, which revealed that the concentrations of SO_2, CO and CH_4 had decreased in the flue gas, while NO_2 had increased (Figure 33). These findings correspond well with the findings discussed in section *4.6 Fuel and additives*, *i.e.* a reversal of trends was observed when SO_2 was added to the combustion zone. This was concluded to be due to a change of SO_2 gas tube, which agrees well with the time of the disturbance.

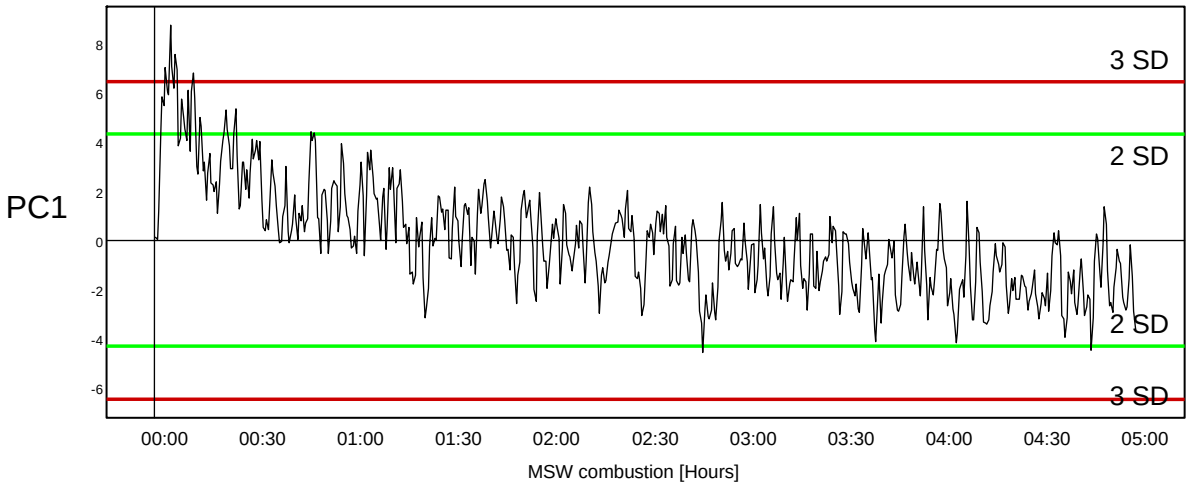

Figure 31. MSPC chart for run 3 (baseline) showing stable combustion performance, without sudden changes, and that steady state occurs after about 2 hours of MSW incineration.

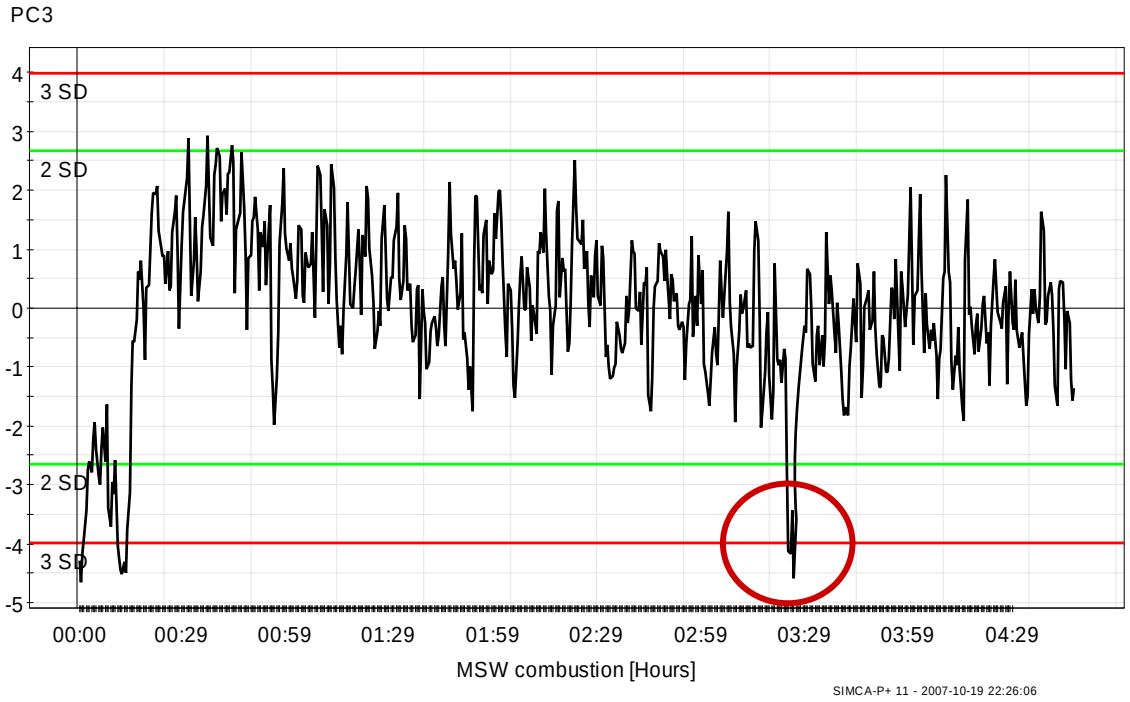

Figure 32. MSPC chart for run 20 (3.9% S in the fuel) showing a disturbance after ca. 3.5 hours of MSW incineration.

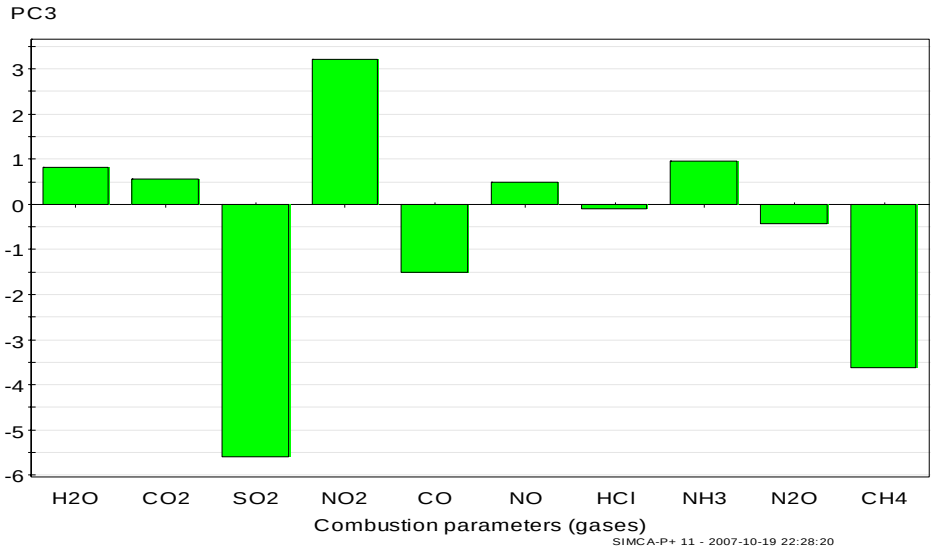

Figure 33. Score contribution plot for run 20 (3.9% S in the fuel) at elapsed time of ca. 3 h 29 min. The plot shows decreases in SO_2, CO and CH_4 and an increase in NO_2 levels in the flue gas due to the disturbance.

4.9.2 Orthogonal partial least squares – O-PLS

The data used in construction of the MVDA table are presented in Tables 14-19 in Appendix 1. The information includes sampling temperatures, residence times, Particulate Matter content, ash distribution and CEM data.

The first (PC1 versus PC2) score and loading plots (Figure 34) identified factors that influence dioxin formation from the following runs and parameters:

- Run 3B – transient condition: identified as an outlier indicated to have a large influence on dioxin formation. The parameters with the greatest effect on the run were CH_4, NH_3 and CO. The score contribution plot (Figure 37, Appendix 3) showed that these parameters were greater in this run than in average runs.
- Run 17 –1.7% Cl level in the fuel: identified as a moderate outlier having a relatively large influence on dioxin formation. The parameters with the greatest effect on the run were NO, HCl and NO_2 levels. The score contribution plot (Figure 38, Appendix 3) showed that these parameters were greater in this run than in average runs. The score contribution plot also revealed that the total amount of ash was less in this run compared to other runs, but this was probably due to losses during collection.
- Run 20 – addition of SO_2 (3.9% S in the fuel): identified as a moderate outlier having a relatively large influence on dioxin formation. The parameters with the greatest effect on the run were SO_2, SO_2:HCl ratio and N_2O. The score contribution plot (Figure 39, Appendix 3) showed that SO_2 and SO_2:HCl ratio increased and NO_2 decreased in this run compared to the average runs. The score contribution plot also revealed that HCl and N_2O levels increased and the temperatures in the bed (combustion zone) decreased in this run.
-

The second (PC2 versus PC3) score and loading plots (Figure 35) identified the following runs and parameters as major factors influencing variations in dioxin formation:

- Run 22 – reduced O_2-level (3.4% O_2) in the flue gas: identified as an outlier with a large influence on dioxin formation. The parameter with the greatest effect on the run was PM (particulate matter). The score contribution plot (Figure 40, Appendix 3) showed that the PM was greater in this run than in the average runs. The score contribution plot also revealed that the amount of cyclone ash increased and O_2, N_2O, NO and NO_2 levels decreased in this run.
- Run 13 – decreased temperature in the freeboard (660 °C): identified as a moderate outlier having a relatively large influence on dioxin formation. The parameters with the greatest effect on the run were N_2O, NO, NO_2 and O_2 levels. The score contribution plot (Figure 42, Appendix 3) showed that NO, N_2O and (especially) NO_2 levels were increased. The O_2 level was unaffected in this run compared to the average runs. The score contribution plot also revealed that the temperatures in the secondary-combustion zone (T3), the freeboard (T4 and T5) and the beginning of the convector (T6) decreased in this run.

- Run 14 – increased temperature in the freeboard (950 °C): identified as a moderate outlier having a relatively large influence on dioxin formation. The parameters with the greatest effect on the run were the temperatures in the freeboard *i.e.* T4 and T5. The score contribution plot (Figure 41, Appendix 3) showed that these parameters increased in this run compared to the average runs. The score contribution plot also revealed that the temperatures in the secondary-combustion zone (T3) and in the beginning of the convector (T6) increased and that N_2O levels decreased in this run.
- Run 17 – see above.
- Run 20 – see above.

The Y-variables, *i.e.* PCDD/PCDF, I-TEQ, sum DIN-PCB, planar PCB and HCB, were located close to each other, indicating that they were correlated to each other.

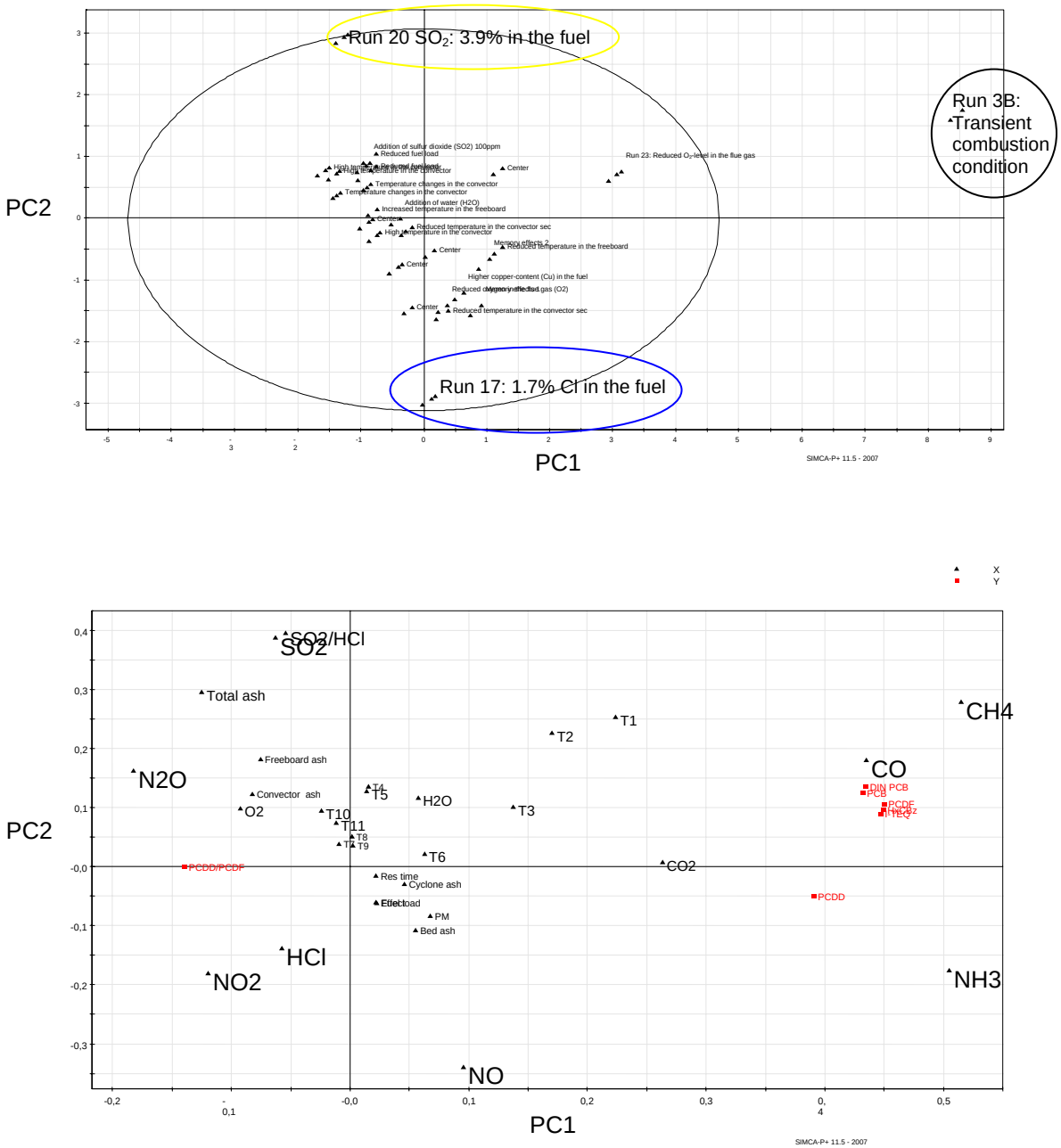

Figure 34. Score (above) and loading (below) plots of the first (PC1) versus second (PC2) components.

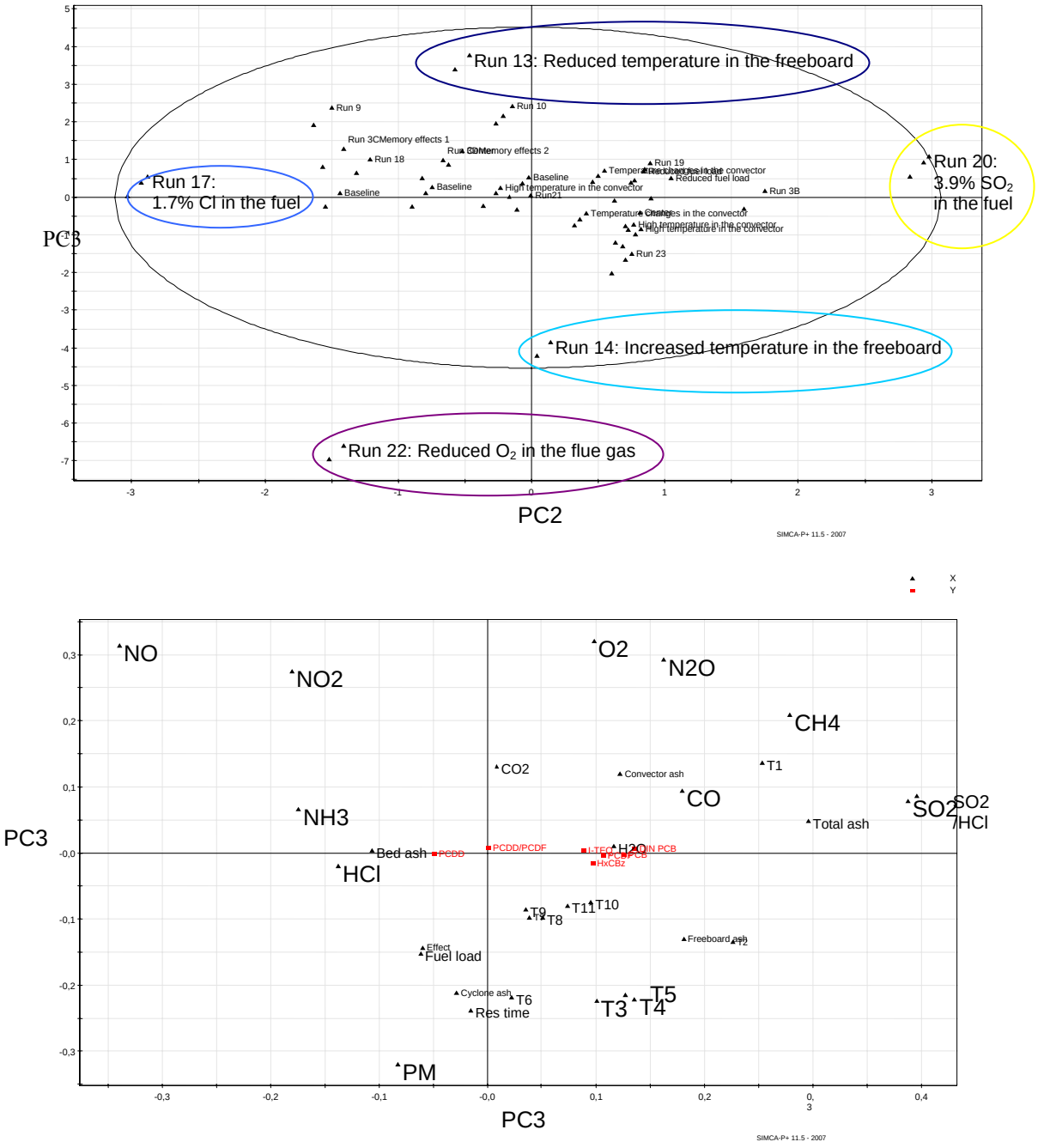

Figure 35. Score (above) and loading (below) plots of the second (PC2) versus third (PC3) components.

5. Conclusions and Summary of Key Findings

5.1. Conclusions

The aim of the study was to identify combustion parameters that substantially affect the formation of dioxins during MSW incineration, in order to find ways to reduce their levels in the flue gas, and thus in flue gas cleaning residues. The study focused mainly on PCDD/F formation, but PCBs and HCB were also considered. The dioxins were sampled simultaneously at three different locations in the post-combustion zone of a laboratory-scale fluidized-bed reactor.

The parameter found to have the largest influence on the reduction of dioxins in the flue gas was:

- Sulphur level in the fuel: An increase in the SO_2:HCl ratio (by mass) from 0 to 0.4 reduced dioxin formation by 70%. A further increase in the SO_2:HCl ratio to 1.6 did not result in a significant difference in reduction at 400 °C. A large increase in SO_2 from <0.5 to 570 ppm in the flue gas (SO_2:HCl ratio, 1.6) resulted in elevation of the CH_4 level and (hence) a smaller reduction (40% rather than 70%) at 200 °C than with a sulphur concentration of 130 ppm (SO_2:HCl ratio 0.4) in the flue gas.

The parameters found to have the largest influence on the formation of dioxins in the flue gas were:

- Transient combustion conditions or incomplete combustion: an increase in CO concentration from < 3 ppm (O_2=11%) to 1600 ppm (O_2=9%) resulted in the dioxin level increasing by about 150-fold. A decrease in the O_2 level (from 10.9% to 2.4%) applied simultaneously with an increase in CO concentration (from < 3 ppm to 1250 ppm) resulted in a seven-fold increase in the dioxin level. Transient combustion conditions were indicated by increases in the CO and CH_4 concentrations in the flue gas. However, the CO and CH_4 levels did not correlate with dioxin formation, since the dioxin concentration in the flue gas was elevated for some time after the transient combustion conditions ended.
- Chlorine level in the fuel: increasing the chlorine level in the fuel from 0.7% to 1.7% resulted in a ten-fold increase in the dioxin levels. An increase in HCl concentration in the flue gas, due to increased chlorine level in the fuel, did not imply on increased dioxin formation since addition of sulphur also increased the HCl concentration. The SO_2:HCl ratio (*e.g.* by mass) is a better parameter to use to optimise the reduction of dioxin formation.
- Freeboard temperature: decreasing the temperature from 800 °C to 660 °C resulted in a three-fold increase in the dioxin concentration.

The effects on dioxin formation of residence times and temperatures in the post-combustion zone were investigated. No high-temperature (640 °C) formation was detected. Under the experimental conditions applied in this study, the greatest formation

appeared to occur between 400 and 300 °C, with indications that the amount and size of particulate matter exerted an effect. The results also suggested that shorter residence times at these temperatures led to lower dioxin levels. HCB and planar PCB (dioxin-like PCB) concentrations were correlated with the dioxin I-TEQ levels, while DIN-PCB concentrations seemed to be unaffected by all parameters except incomplete combustion.

5.2. Summary of Key Findings and their Implications

In summary, this study confirms previous findings that:

- Little PCDD/F is found immediately downstream an efficient incineration process which is operating at high temperature, low CO-levels and excess air.
- Formation of PCDD/F takes place in the post combustion section, corresponding to the convection part of a Waste-to-Energy boiler, and the formation increases with the residence time in this section
- Poor combustion detected as high CO level significantly increases PCDD/F-formation
- Sulphur, forming SO_2, has an inhibiting effect on PCDD/F formation
- Presence of chlorine increases the formation of PCDD/F.
- The PCDD/F baseline level of around 0.5-1 ng/m³ (I-TEQ) detected at the outlet of the pilot scale reactor system is within the interval (in the low end) of what is detected in the raw flue gas of a typical Waste-to-Energy incinerator/boiler system.

Due to the standardised environment in the pilot scale reactor system used for the experiments, the study contributes with new knowledge particularly by quantifying some of the above mentioned effects, narrowing the temperature window for PCDD/F formation and indicating the presence of memory effect in the post combustion part of the boiler.

New findings thus include:

- Formation of PCDD/F particularly takes place in the narrow temperature interval 300-400 °C. Little, if any, formation takes place in the convection part below 300 °C.
- Formation of PCDD/F increases with residence time in the temperature range 300-500 °C
- The inhibiting effect of sulphur is found to be 70% reduction of PCDD/F level by SO_2:HCl molar ratio of 0.4 (compared to baseline results with undetectable SO_2). Increasing the molar ratio to 1.6 had no further effect.
- Increasing the HCl content by factor 2.4 to a level of 900 mg/Nm³ (dry flue gas at 11% O_2), increased the PCDD/F formation by factor 10.
- The occurrence of transient conditions increases the PCDD/F formation dramatically, for instance a CO-peak of 1600 ppm (2000 mg/Nm³) caused the PCDD/F level to increase by factor 150.
- Such an occurrence was accompanied by memory effect where elevated PCDD/F level was detected for several hours after the CO-peak.

The practical implications of the results for the design and operation of Waste-to-Energy furnace/boiler systems include:

- Formation of PCDD/F in Waste-to-Energy systems (and probably other commercial boilers) can be minimised by avoiding transient conditions, i.e. avoiding CO-peaks and ensuring low CO-levels.
- Formation of PCDD/F is minimised by reducing the flue gas residence time in the temperature interval 300-500 °C.
- PCDD/F formation may to some extent be controlled by ensuring presence of SO_2 in the boiler, probably at a level corresponding to SO_2:HCl molar ratio of around 0.4 (mass ratio 0.7). This may be ensured by mixing waste properly, thereby smoothing out the SO_2-level, or by controlled addition of waste fractions known to be high in sulphur, e.g. containing gypsum or tyres.
- Measurement of PCDD/F in the raw flue gas of Waste-to-Energy systems (and other commercial boilers) and verification of results should take the memory effect from transient operation into account by sampling only when the operational status of the facility is well established and documented to reflect the desired operation for many hours (or days) preceding sampling.
- The results contribute to input data needed for establishing and fitting a PCDD/F-generation model for subsequent use in a CFD-model for a furnace/boiler system. Such a model provides a modern flow simulation tool for optimising the design of boilers to minimise PCDD/F formation and maintaining the energy output.

7. Literature Cited

(1) Olie, K.; Vermeulen, P. L.; Hutzinger, O. Chlorodibenzo-p-dioxins and chlorodibenzofurans are trace components of fly ash and flue gas of some municipal incinerators in the netherlands. *Chemosphere*. **1977**, *8* 455-459.

(2) European Union Council Directive 2000/76/EG. . **2007**.

(3) Council regulation (EC) No 1195/2006 amending Annex IV to regulation (EC) No 850/2004 of European Parliament and of the Council on persistent orgnic pollutants. *Official Journal of the European Union*. **2006**.

(4) van den Berg, M.; Birnbaum, L.; Boseveld, A. T. C.; Brunström, B.; Cook, P.; Feeley, M.; Giesy, J. P.; Hanberg, A.; Hasegawa, R.; Kennedy, S. W.; Kubiak, T.; Larsen, J. C.; van Leeuwen, F. X. R.; Liem, A. K. D.; Nolt, C.; Peterson, R. E.; Poellinger, L.; Safe, S.; Schrenk, D.; Tillitt, D.; Tysklind, M.; Younes, M.; Waern, F.; Zacharewski, T. Toxic equivalency factors (TEFs) for PCBs, PCDDs, PCDFs for humans and wildlife. *Environ Health Perspect*. **1998**, *106* 775-792.

(5) European Committee for Standardization Determination of PCBs and related products. *DIN EN*. **200**, *12766:1-2* .

(6) Birgerson, B.; Sterner, O.; Zimerson, E. Kemiska hälsorisker Toxikologi I kemiskt perspektiv. *Malmö: Liber-Hermods*. **1995**, *ISBN 91-23-01731-7* .

(7) Shaub, W. M.; Tsang, W. Dioxin Formation in Incinerators. *Environmental Science & Technology*. **1983**, *17* 721-730.

(8) Vogg, H.; Stieglitz, L. Thermal behavior of PCDD/PCDF in fly ash from municipal incinerators. *Chemosphere*. **1986**, *15* (9-12), 1373-1378.

(9) Stieglitz, L.; Zwick, G.; Beck, J.; Roth, W.; Vogg, H. On the *de-novo* synthesis of PCDD/PCDF on fly ash of municipal waste incinerators. *Chemosphere*. **1989**, *18* (1-6), 1219-1226.

(10) Karasek, F. W.; Dickson, L. C. Model Studies of Polychlorinated Dibenzo-*p*-Dioxin Formation During Municipal Refuse Incineration. *Science*. **1987**, *237* 754-756.

(11) Huang, H.; Buekens, A. On the mechanisms of dioxin formation in combustion processe. *Chemosphere*. **1995**, *31* (9), 4099-4117.

(12) Griffin, R. D. A new theory of dioxin formation in municipal solid waste combustion. *Chemosphere*. **1986**, *15* (9-12), 1987-1990.

(13) Gullet, B. K.; Bruce, K. R.; Beach, L. O. The effect of metal catalysts on the formation of polychlorinated bibenzo-p-dioxin and polychlorinated dibenzofuran precursors. *Chemosphere*. **1990**, *20* (10-12), 1945-1952.

(14) Gullett, B. K.; Bruce, K. R.; Beach, L. O. Effect of sulfur dioxide on the formation mechanism of polychlorinated dibenzodioxin and dibenzofuran in municipal waste combustors. *Environmental Science & Technology*. **1992**, *26* (10), 1938-1943.

(15) Lundin, L.; Aurell, J.; Marklund, S. Fate of PCDD and PCDF during thermal treatment of waste incineration ash. *Manuscript*. **2008**.

(16) Wikström, E.; Löfvenius, G.; Rappe, C.; Marklund, S. Influence of Level and Form of Chlorine on the Formation of Chlorinated Dioxins, Dibenzofurans, and Benzenes during Combustion of an Artificial Fuel in a Laboratory Reactor. *Environmental Science & Technology*. **1996**, *30* (5), 1637-1644.

(17) Luijk, R.; Akkerman, D. M.; Slot, P.; Olie, K.; Kapteijn, F. Mechanism of formation of polychlorinated dibenzo-p-dioxins and dibenzofurans in the catalyzed combustion of carbon. *Environmental Science & Technology*. **1994**, *28* 312-321.

(18) Hatanaka, T.; Kitajima, A.; Takeuchi, M. Role of copper chloride in the formation of polychlorinated dibenzo-p-dioxins and dibenzofurans during incineration. *Chemosphere*. **2004**, *57* 73-79.

(19) Gullett, B. K.; Raghunathan, K.; Dunn, J. E. The effect of cofiring high-sulfur coal with municipal waste on formation of polychlorinated dibenzodioxin and polychlorinated dibenzofuran. *Environmental engineering science*. **1998**, *15* (1), 59-70.

(20) Ogawa, H.; Orita, N.; Horaguchi, M.; Suzuki, T.; Okada, M.; Yasuda, S. Dioxin reduction by sulfur component addition. *Chemosphere*. **1996**, *32* (1), 151-157.

(21) Chang, M. B.; Cheng, Y. C.; Chi, K. H. Reducing PCDD/F formation by adding sulfur as inhibitor in waste incineration processes. *Science of the Total Environment*. **2006**, *366* 456-465.

(22) Hunsinger, H.; Seifert, H.; Jay, K. Reduction of PCDD/F formation in MSWI by a process-integrated $SO_{2\ cycle}$. *IT3-Conference*. **2006**, *May 15-19* .

(23) Lenoir, D.; Kaune, A.; Hutzinger, O.; Mutzenich, G.; Horch, K. Influence of operating parameters and fuel type on PCDD/F emissions from a fluidized bed incinerator. *Chemosphere*. **1991**, *23* (8-10), 1491-1500.

(24) Stieglitz, L.; Zwick, G.; Beck, J.; Bautz, H.; Roth, W. The role of particulate carbon in the de-novo synthesis of polychlorinated dibenzodioxins and -furans in fly-ash. *Chemosphere*. **1990**, *20* (10-12), 1953-1958.

(25) Jay, K.; Stieglitz, L. On the mechanism of formation of polychlorinated aromatic compounds with copper(II) chloride. *Chemosphere*. **1991**, *22* (11), 987-996.

(26) Ruokojärvi, P. H.; Asikainen, A.; Ruuskanen, J.; Tuppurainen, K. A.; Mueller, C.; Kilpinen, P.; Yli-Keturi, N. Urea as a PCDD/F inhibitor in municipal waste incineration. *Journal of the Air &Waste Management Association*. **2001**, *51* (March), 422-431.

(27) Fängmark, I.; Strömberg, B.; Berge, N.; Rappe, C. The influence of post combustion temperature profiles on the formation of PCDDs, PCDFs, PCBzs and PCBs in a pilot incinerator. *Environmental Science & Technology*. **1994**, *28* 624-629.

(28) Wikström, E.; Marklund, S. Secondary formation of chlorinated dibenzo-p-dioxins, dibenzofurans, bipehnyls, benzenes, and phenols during MSW combustion. *Environmental Science & Technology*. **2000**, *34* 604-609.

(29) Hatanaka, T.; Imagawa, T.; Kitajima, A.; Takeuchi, M. Effects of combustion temperature on PCDD/Fs formation in laboratory-scale fluidized-bed incinerator. *Environmental Science & Technology*. **2001**, *35* 4936-4940.

(30) Blumenstock, M.; Zimmerman, R.; Schramm, K.-W.; Kettrup, A. Influence of combustion conditions on the PCDD/F-, PCB-, PCBz- and PAH-concentrations in the post-combustion chamber of a waste incineration pilot plant. *Chemosphere*. **2000**, *40* 987-993.

(31) Niessen, W. R. Combustion and incineration processes 3rd ed. *Marcel Dekker, Inc. :New York*. **2002**, (ISBN: 0-8247-0629-3).

(32) Vogg, H.; Metzger, M.; Stieglitz, L. Recent findings on the formation and decomposition of PCDD/PCDF in municipal solid waste incineration. *Waste Management & Research*. **1987**, *5* 285-294.

(33) Hunsinger, H.; Seifert, H.; Jay, K. Formation of PCDD/F during start-up of MSWI. *Organohalogen compounds*. **2003**, *60-65* .

(34) Leclerc, D.; Duo, W. L.; Vessey, M. Effects of combustion and operating conditions on PCDD/PCDF emissions from power boilers burning salt-laden wood waste. *Chemosphere*. **2006**, *63* 676-689.

(35) Oh, J.-E.; Gullett, B. K.; Ryan, S.; Touati, A. Mechanistic relationships among PCDD/Fs, PCNs, PAHs, ClPhs, and ClBzs in municipal waste incineration. *Environmental Science & Technology*. **2007**, *41* 4705-4710.

(36) Weber, R.; Sakurai, T.; Ueno, S.; Nishino, J. Correlation of PCDD/PCDF and CO values in a MSW incinerator-indication of memory effects in the high temperature/cooling section. *Chemosphere*. **2002**, *49* 127-134.

(37) Wikström, E.; Marklund, S.; Tysklind, M. Influence of Variation in Combustion Conditions on the Primary Formation of Chlorinated Organic Micropollutants during Muncipal Waste Combustion. *Environ. Sci. Technol.* **1999**, *33* 4263-4269.

(38) Neur-Etscheidt, K.; Nordsieck, H. O.; Liu, Y.; Kettrup, A.; Zimmerman, R. PCDD/F and other micropollutants in MSWI crude gas and ashes during plant start-up and shut-down processes. *Environmental Science & Technology*. **2006**, *40* 342-349.

(39) Wikström, E.; Andersson, P.; Marklund, S. Design of a laboratory scale fluidized bed reactor. *Review of Scientific Instruments*. **1998**, *69* 1850-1859.

(40) Wikström, E.; Marklund, S. Combustion of an artificial municipal solid waste in a laboratory fludised bed reactor. *Waste Management & Research*. **1998**, *16* (4), 342-350.

(41) European Committee for Standardization. Stationary source emissions - Determination of the mass concentration of PCDDs/PCDFs. *EN*. **1997**, *1948:1-3* .

(42) Swedish Standard Stationary source emissions - Determination of low range mass concentration of dust - Part 1:Manual gravimetric method. *SS:EN*. **2001**, *13284-1* .

(43) Liljelind, P.; Söderström, G.; Hedman, B.; Karlsson, S.; Lundin, L.; Marklund, S. Method for multiresidue determination of halogenated aromatics and PAHs in combustion-related samples. *Environmental Science & Technology*. **2003**, *37* (16), 3680-3686.

(44) Jolliffe, I. T. Principal component analysis. *Sringer, ISBN 0-387-96269-7*. **1986**.

(45) Wold, S. Principal Component Analysis. *Chemometrics and Intelligent Laboratory Systems*. **1987**, *2* 37-52.

(46) Trygg, J.; Wold, S. Orthogonal projections to latents structures (O-PLS). *Journal of chemometrics*. **2002**, *2002* (16), 119-128.

Appendix 1

Table 14. Dioxin (in I-TEQ and sum PCDD/F), PCB and HCB concentrations in the flue gas, in ng/Nm^3 dg 11% O_2.

Run	Experiment	Sampling Temp. °C	I-TEQ	Sum PCDF	Sum PCDD	Ratio PCDD/PCDF	Sum DIN PCB	planar PCB	HCB
1:2	Baseline	P4=300	0.79	34	4	0.12	9	0.45	91
1:3		P7=200	1.3	54	7	0.13	26	1.5	124
2:2	Baseline	P4=300	0.57	24	3	0.13	10	0.34	66
2:3		P7=200	0.61	27	3	0.11	12	0.85	144
3:2	Baseline	P4=300	0.89	38	4	0.11	44	0.26	19
3:3		P7=200	0.71	33	3	0.09	23	0.60	75
4:1	Baseline	P3=400	0.60	23	3	0.11	22	0.21	55
4:2		P4=300	0.43	18	2	0.11	14	0.15	56
4:3		P7=200	0.46	19	2	0.10	10	0.25	87
5:1	Baseline	P3=400	0.66	24	3	0.13	18	0.20	42
5:2		P4=300	0.59	24	3	0.12	19	0.24	65
5:3		P7=200	0.50	21	2	0.11	11	0.26	80
6:1	High temperature in	P3=460	0.15	6	0.5	0.08	7	0.07	10
6:2	the convector	P4=360	0.19	7	1	0.14	16	0.15	45
6:3		P7=260	0.76	27	6	0.21	20	1.4	251
7:1	High temperature in	P3=460	0.16	7	0.4	0.05	8	0.06	169
7:2	the convector	P4=360	0.21	8	1	0.10	31	0.12	27
7:3		P7=260	0.57	21	3	0.17	28	0.83	204
8:1	High temperature in	P3=460	0.20	7*	0.4*	0.05*	6	0.08	10
8:2	the convector	P4=360	0.22	8*	1*	0.10*	15	0.11	29
8:3		P7=260	0.33	12*	1*	0.12*	28	0.36	79
9:2	Reduced temperature	P4=200	0.36	15	2	0.13	8	0.15	67
9:3	in the convector section	P7=100	0.22	11	1	0.09	7	0.33	80
10:1	Reduced temperature	P2=640	<0.01	<0.1[a]	<0.1[a]	-	13	0.03	2
10:2	in the convector	P3=300	0.50	16*	1.7*	0.10*	30	0.43	170
10:3	section	P4=200	0.37	12*	1.3*	0.10*	12	0.34	167
11:1	Temperature changes	P3=400	0.47	18	1.5	0.09	6	0.14	41
11:2	in the convector	P4=333	0.32	13	1.2	0.09	32	0.13	71
11:3		P5=300	0.42	17	1.8	0.11	12	0.22	114
12:1	Temperature changes	P3=400	0.43	16	1.7	0.10	9	0.13	34
12:2	in the convector	P4=333	0.50	21	2.1	0.10	12	0.18	83
12:3		P5=300	0.66	27	2.8	0.10	17	0.26	104
13:2	Reduced temperature	P4=300	2.2	88	10	0.11	19	1.2	146
13:3	in the freeboard (660°C)	P7=200	1.7	67	8	0.12	24	1.3	147

14:2	Increased temperature	P4=300	0.74	28	5	0.18	52	0.26	101
14:3	in the freeboard (950°C)	P7=200	0.71	29	4	0.14	14	0.74	132
15:2	Reduced fuel load	P4=300	0.46	20	7	0.35	15	0.52	95
15:3	0.68 kg/h	P7=200	3.8	127	76	0.60	23	6.8	966
16:1	Reduced fuel load	P3=400	0.14	5	0.5	0.10	43	0.09	14
16:2	0.60 kg/h	P4=300	0.12	5	0.5	0.10	38	0.08	24
16:3		P7=200	0.12	4	0.6	0.13	33	0.14	33
17:1	Higher chlorine-	P3=400	5.8	172	50	0.29	16	2.0	607
17:2	content (Cl) in the fuel	P4=300	7.5	218	67	0.31	25	2.9	928
17:3	1.7% Cl	P7=200	6.1	186	50	0.27	28	3.7	794
18:2	Higher copper-content	P4=300	0.30	13	2	0.15	15	0.22	79
18:3	(Cu) in the fuel 0.011%	P7=200	0.43	19	2	0.11	17	0.62	114
19:1	Addition of sulfur	P3=400	0.20	7	1	0.12	11	0.09	39
19:2	dioxide (SO_2)	P4=300	0.22	8	1	0.14	22	0.10	49
19:3	1.9% S in the fuel	P7=200	0.16	8	2	0.21	12	0.26	85
20:1	Addition of sulfur	P3=400	0.12	4	1	0.17	53	0.07	15
20:2	dioxide (SO_2)	P4=300	0.22	7	2	0.24	12	0.25	19
20:3	3.9% in the fuel	P7=200	0.34	12	4	0.33	8	0.48	31
21:2	Addition of water	P4=300	0.46	17	3	0.18	27	0.30	20
21:3	(H_2O)	P7=200	0.94	39	5	0.13	16	0.88	65
22:2	Reduced oxygen in the	P4=300	4.3	231	30	0.13	22	3.9	386
22:3	flue gas (O_2) (3.4%)	P7=200	4.1	247	37	0.15	26	6.6	648
23:1	Reduced oxygen in the	P3=400	2.39	106	7	0.06	15	2.1	190
23:2	flue gas (O_2) (2.45)	P4=300	2.20	99	7	0.07	10	2.0	185
23:3		P7=200	2.67	130	10	0.07	11	2.8	308
3:B:2	Transient condition	P4=300	109	4994	273	0.05	615	150	7749
3:B:3		P7=200	97	4402	241	0.05	551	248	6908
3:C:2	Memory effects 1	P4=300	28	1078	151	0.14	161	35	1332
3:C:3		P7=200	37	1452	211	0.14	182	59	1342
3:D:2	Memory effects 2	P4=300	3.9	195	23	0.12	33	4.1	310
3:D:3		P7=200	6.6	306	41	0.13	43	9.1	425

[*] Hepta- and octa- CDF and CDD are not included due to contamination. However, the I-TEQ value is not affected.
[a] Non detect.

Results from experimental campaign, samples from P2 not presented due to sample defect.

Table 15. Average flue gas value during sampling, dry gas (except for H_2O).

Run	Experiment	H_2O	CO_2	SO_2	NO_2	CO	NO	HCl	NH_3	N_2O	CH_4	O_2
		%	%	ppm	ppm	ppm	ppm	ppm	ppm	ppm	ppm	%
1	Baseline	9.0	10.7	<0.5	27	2.1	450	254	0.6	39	<0.5	9.8
2	Baseline	8.3	9.9	<0.5	32	2.8	506	244	0.5	52	<0.5	10.9
3	Baseline	8.2	9.6	<0.5	35	2.8	500	222	0.2	50	<0.5	10.9
4	Baseline	7.1	7.7	<0.5	30	2.1	390	158	0.7	45	<0.5	11.8
5	Baseline	7.6	8.9	<0.5	32	2.8	446	212	0.5	49	<0.5	10.1
6	High temperature in the convector	6.7	7.2	<0.5	39	1.5	349	199	1.0	46	<0.5	11.5
7	High temperature in the convector	7.0	7.6	<0.5	39	2.5	377	200	0.6	48	<0.5	11.6
8	High temperature in the convector	8.0	9.6	<0.5	38	3.1	476	256	0.4	56	<0.5	10.6
9	Low temperature in the convector	8.1	9.5	<0.5	30	2.8	503	261	0.2	54	<0.5	11.2
10	Low temperature in the convector	7.5	8.6	<0.5	28	2.8	474	229	0.1	57	<0.5	11.6
11	Temperature changes in the convector	7.3	8.2	<0.5	37	2.0	431	165	0.7	57	<0.5	12.4
12	Temperature changes in the convector	6.6	6.9	<0.5	30	1.7	364	139	0.5	44	<0.5	11.3
13	Reduced temperature in the freeboard	8.5	10.2	<0.5	46	40	462	262	0.8	53	<0.5	10.5
14	Increased temperature in the freeboard	7.5	8.7	<0.5	31	2.3	433	191	0.6	7.5	<0.5	10.9
15	Reduced fuel load	7.7	8.9	<0.5	20	1.8	354	259	0.4	51	<0.5	11.3
16	Reduced fuel load	7.0	7.6	<0.5	39	2.5	378	200	0.6	48	<0.5	11.0
17	Increased Cl-level in the fuel	7.6	9.2	<0.5	32	3.4	502	538	0.6	53	<0.5	11.2
18	Increased Cu-level in the fuel	8.0	9.5	<0.5	38	3.7	607	187	0.4	36	<0.5	11.1
19	Addition of SO_2	7.6	9.0	131	12	2.9	409	319	0.5	77	<0.5	11.4
20	Addition of SO_2	7.7	9.3	572	10	3.9	405	366	1.4	76	2.6	10.0
21	Addition of H_2O	21	10.0	<0.5	27	3.2	476	236	0.8	75	<0.5	10.9
22	Reduced O_2-level in the flue gas	7.4	8.6	1.2	5.4	550	317	92	15	18	54	3.4
23	Reduced O_2-level in the flue gas	7.7	8.6	5.0	4.2	1254	261	166	21	32	130	2.4
3:B	Transient conditions	9.5	11.3	16	14	1577	465	213	34	29	247	8.8
3:C	Memory effects 1	7.9	9.3	<0.5	32	42	530	229	13	47	5	11.3
3:D	Memory effects 2	8.5	10.1	<0.5	34	2.4	532	251	5.1	44	<0.5	10.4

Table 16. Average temperatures during sampling, in °C.

Run	Experiment	T1	T2	T3	T4	T5	T6	T7	T8	T9	T10	T11
1	Baseline	856	841	781	805	803	631	386	332	253	222	204
2	Baseline	825	806	750	802	802	640	395	330	255	225	207
3	Baseline	822	802	749	802	802	638	400	334	260	224	209
4	Baseline	818	811	756	802	802	642	406	330	252	221	205
5	Baseline	818	813	757	803	802	639	400	335	256	221	206
6	High temperature in the convector	824	824	768	802	802	650	468	400	321	295	265
7	High temperature in the convector	822	822	766	802	802	643	465	407	323	291	265
8	High temperature in the convector	814	809	757	802	802	649	476	409	323	279	260
9	Low temperature in the convector	812	802	750	802	802	634	318	217	157	103	103
10	Low temperature in the convector	810	807	756	802	802	616	324	246	160	204	163
11	Temperature changes in the convector	810	820	768	802	802	637	403	344	293	260	234
12	Temperature changes in the convector	819	818	762	802	802	634	403	344	293	260	230
13	Reduced temperature in the freeboard	836	823	736	660	655	545	399	332	255	222	207
14	Increased temperature in the freeboard	824	830	811	950	952	728	398	330	256	225	208
15	Reduced fuel load	829	813	740	802	802	607	403	332	256	226	207
16	Reduced fuel load	823	825	760	801	802	622	407	335	259	229	212
17	Increased Cl-level in the fuel	809	813	761	803	803	644	408	331	257	225	210
18	Increased Cu-level in the fuel	827	814	760	802	802	629	401	335	259	226	208
19	Addition of SO_2 (1.9%S)	809	808	752	802	802	629	403	332	252	223	204
20	Addition of SO_2 (3.9%S)	803	796	744	803	802	636	403	335	255	225	209
21	Addition of H_2O	796	813	774	803	803	656	396	330	255	225	207
22	Reduced O_2-level in the flue gas	801	838	798	809	807	668	399	330	256	223	204
23	Reduced O_2-level in the flue gas	811	807	760	808	806	650	406	333	255	224	207
3:B	Transient conditions	844	833	779	812	811	651	403	337	262	226	210
3:C	Memory effects 1	815	804	753	802	803	637	401	334	258	224	207
3:D	Memory effects 2	832	819	760	802	802	639	401	334	257	223	206

The temperatures in the sample ports were: P2 = T6, P3 = T8+60°C, P4 = T9+40°C and P7 = T11.

Table 17. Particulate matter levels in the flue gas, fuel loads and additives.

Run	Experiment	Particulate Matter g/Nm^3 11% O_2 dg	Fuel load g/h	Effect kW/h	Added H_2O g/min	Added N_2 l/min	Added 2%-SO_2 l/min
1	Baseline	1.4	1000	5.4	-	-	-
2	Baseline	1.0	900	4.9	-	-	-
3	Baseline	1.4	925	5.0	-	-	-
4	Baseline	1.1	852	4.6	-	-	-
5	Baseline	1.3	900	4.9	-	-	-
6	High temperature in the convector	1.1	843	4.6	-	-	-
7	High temperature in the convector	1.5	954	5.2	-	-	-
8	High temperature in the convector	1.3	864	4.7	-	-	-
9	Low temperature in the convector	1.5	885	4.8	-	-	-
10	Low temperature in the convector	1.3	815	4.4	-	-	-
11	Temperature changes in the convector	1.5	795	4.3	-	-	-
12	Temperature changes in the convector	1.7	837	4.5	-	-	-
13	Reduced temperature in the freeboard	1.4	900	4.8	-	-	-
14	Increased temperature in the freeboard	1.0	925	5.0	-	-	-
15	Reduced fuel load	1.2	675	3.6	-	-	-
16	Reduced fuel load	1.6	593	3.2	-	-	-
17	Increased Cl-level in the fuel	0.9	813	4.4	-	-	-
18	Increased Cu-level in the fuel	1.7	895	4.8	-	-	-
19	Addition of SO_2	1.4	859	4.6	-	-	5.3
20	Addition of SO_2	2.0	886	4.8	-	-	10.7
21	Addition of H_2O	2.4	880	4.8	15	-	-
22	Reduced O_2-level in the flue gas	6.0 (10.6[a])	1020	5.5	-	40	-
23	Reduced O_2-level in the flue gas	0.8 (1.5[a])	849	4.6	-	50	-
3:B	Transient conditions	-	[c]	[c]	-	-	-
3:C	Memory effects 1	-	[c]	[c]	-	-	-
3:D	Memory effects 2	-	[c]	[c]	-	-	-

a Not normalized to 11% O_2. [c] run 3.

Table 18. **Proportions of ash in the bed, convector and cyclone ashes, and total amount of ash as a percentage of the fuel mass.**

Run	Experiment	Bed (%)	Convector (%)	Cyclone (%)	Total (% of fuel)
1	Baseline	18	76	6	14
2	Baseline	15	82	3	13
3	Baseline	22	54	25	13
4	Baseline	5	92	4	12
5	Baseline	15	77	8	12
6	High temperature in the convector	11	83	5	13
7	High temperature in the convector	9	84	7	15
8	High temperature in the convector	14	81	5	13
9	Low temperature in the convector	16	83	0	13
10	Low temperature in the convector	14	83	4	15
11	Temperature changes in the convector	10	85	5	14
12	Temperature changes in the convector	14	77	9	14
13	Reduced temperature in the freeboard	18	79	3	13
14	Increased temperature in the freeboard	12	83	5	13
15	Reduced fuel load	29	70	1	13
16	Reduced fuel load	25	74	1	12
17	Increased Cl-level in the fuel	54	46	0	8
18	Increased Cu-level in the fuel	15	78	7	12
19	Addition of SO_2	18	76	6	13
20	Addition of SO_2	33	62	5	14
21	Addition of H_2O	7	79	14	13
22	Reduced O_2-level in the flue gas	0	68	37	13
23	Reduced O_2-level in the flue gas	14	81	5	13

The proportions of ash in the bed, convector and cyclone ashes were calculated by dividing their amounts by the total amounts collected. The total ash content was calculated by dividing the total mass of ash by the total fuel load to obtain an understanding of the system. The total ash may differ from the ash content calculated from analyses of the fuel (Table 4), due to practical limitations (and losses) in handling.

Table 19. Residence times in the freeboard and between the freeboard and sample ports, in seconds.

Run	Experiment	Freeboard	P2	P3	P4	P5	P7
1	Baseline	5.1			2.4		4.5
2	Baseline	5.1			2.3		4.4
3	Baseline	5.1			2.3		4.4
4	Baseline	5.1		1.4	2.3		4.4
5	Baseline	5.1		1.4	2.3		4.4
6	High temperature in the convector	5.1		1.3	2.1		4.0
7	High temperature in the convector	5.1		1.3	2.1		4.0
8	High temperature in the convector	5.1		1.3	2.1		4.0
9	Low temperature in the convector	5.1			2.7		5.4
10	Low temperature in the convector	5.1	0.1	1.6	2.7		
11	Temperature changes in the convector	5.1		1.4	2.3	3.2	
12	Temperature changes in the convector	5.1		1.4	2.3	3.2	
13	Reduced temperature in the freeboard	5.9			2.4		4.5
14	Increased temperature in the freeboard	4.5			2.3		4.4
15	Reduced fuel load	7.6			3.5		6.6
16	Reduced fuel load	7.2		2.0	3.3		6.4
17	Increased Cl-level in the fuel	5.1		1.4	2.3		4.4
18	Increased Cu-level in the fuel	5.1			2.3		4.4
19	Addition of SO_2	5.1		1.4	2.3		4.4
20	Addition of SO_2	5.1		1.4	2.3		4.4
21	Addition of H_2O	5.1			2.3		4.4
22	Reduced O_2-level in the flue gas	5.1			2.3		4.4
23	Reduced O_2-level in the flue gas	5.1		1.4	2.3		4.4
3:B	Transient conditions	5.1			2.3		4.4
3:C	Memory effects 1	5.1			2.3		4.4
3:D	Memory effects 2	5.1			2.3		4.4

Appendix 2

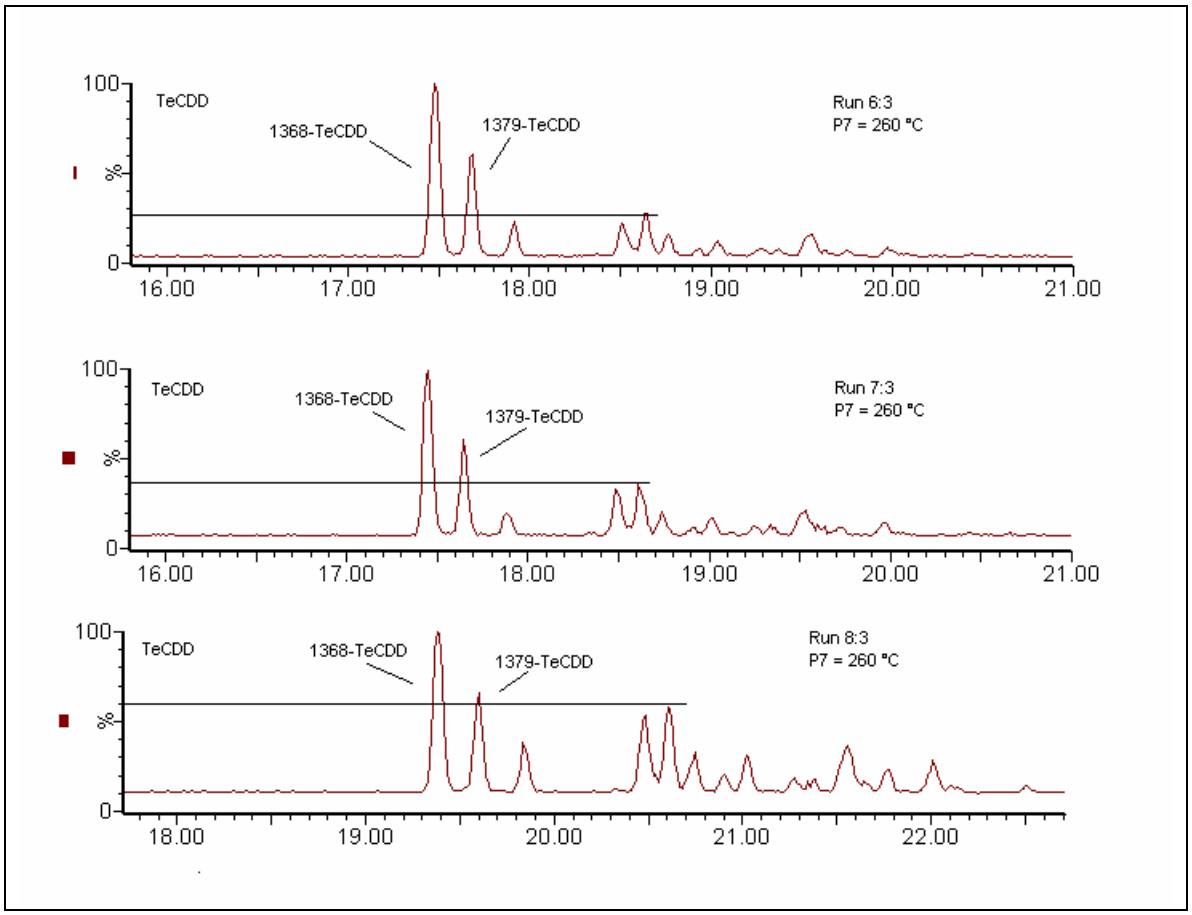

Figure 35. GC-HRMS chromatograms of tetra-chlorinated PCDDs found in runs 6-8, at sampling point P7/260 °C. The y-axis shows the relative abundance on a peak height basis. See Figure 25 for baseline patterns.

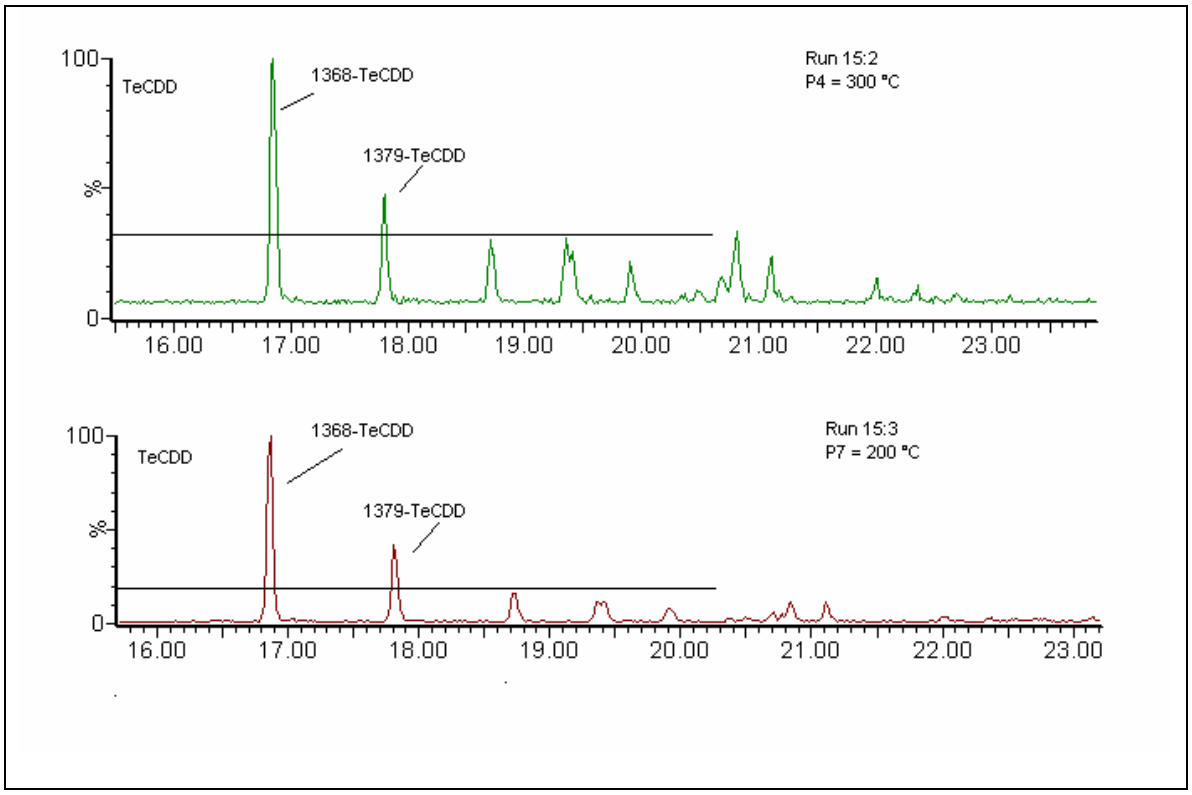

Figure 36. GC-HRMS chromatograms of tetra-chlorinated PCDDs found in runs 15 and 16, sampling points P4/300 °C and P7/200 °C. The y-axis shows the relative abundance on a peak height basis. In this analysis a SP 2330 column was used. See Figure 25 for baseline patterns.

Appendix 3

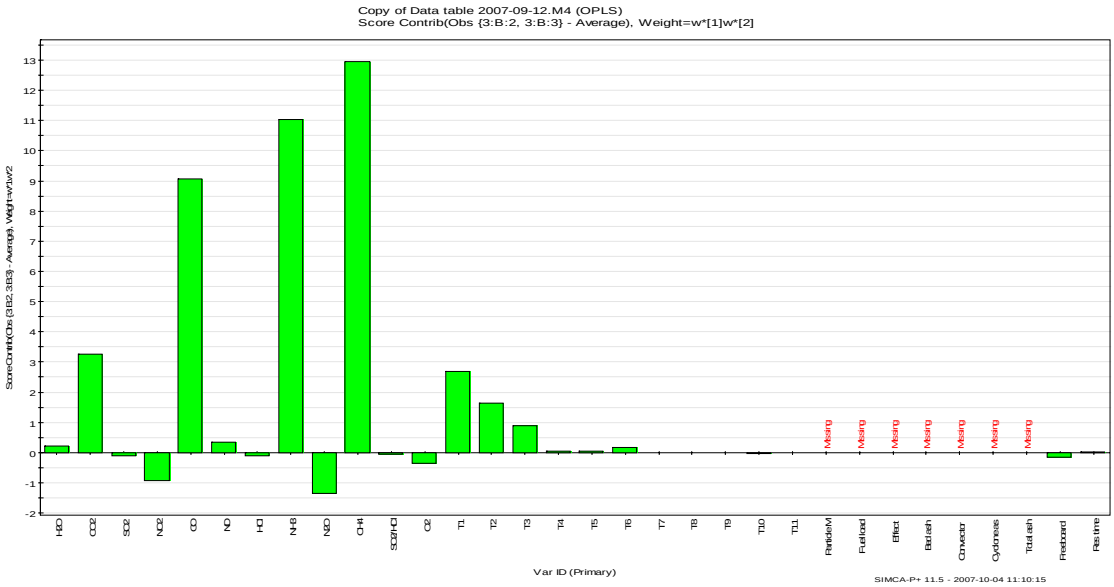

Figure 37. Score contribution plot: Run 3B – transient combustion conditions.

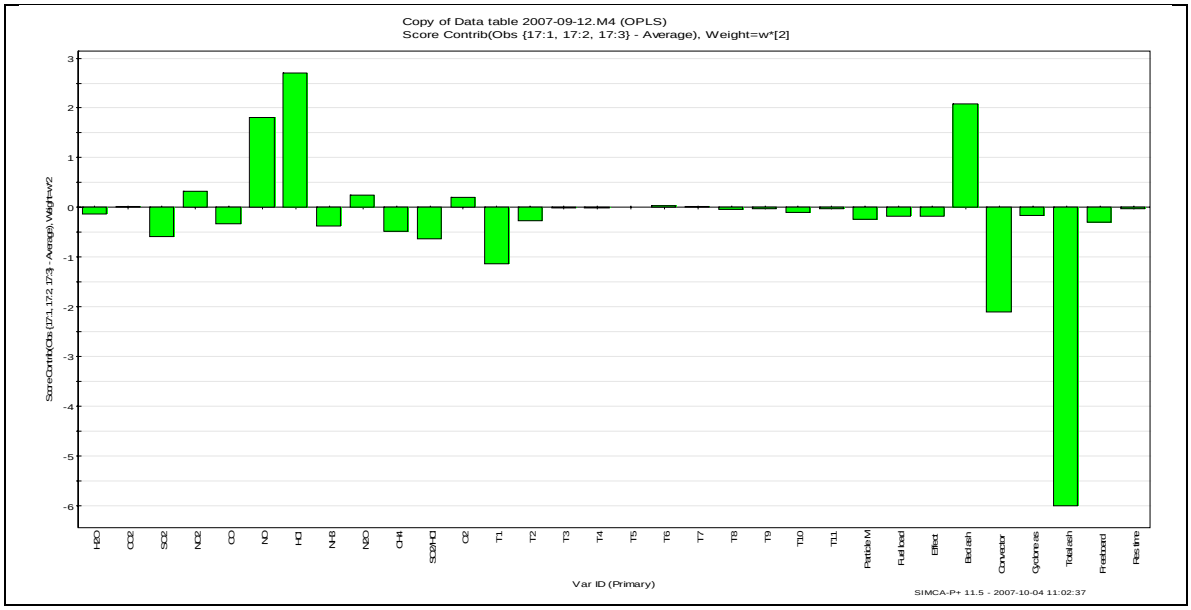

Figure 38. Score contribution plot: Run 17 – increased Cl level in the fuel.

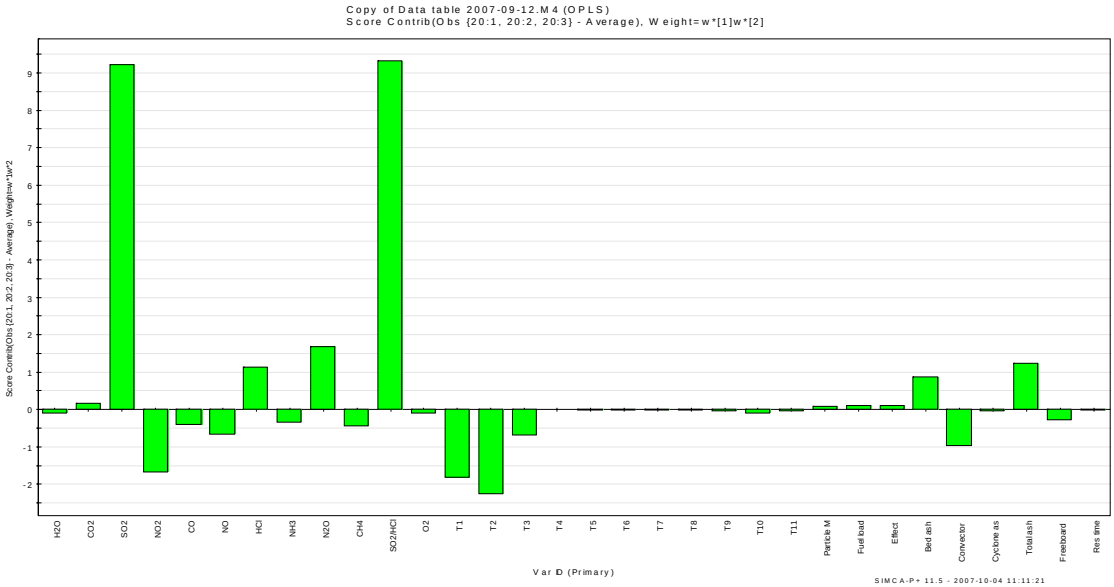

Figure 39. Score contribution plot: Run 20 – SO_2 addition (3.9% in the fuel).

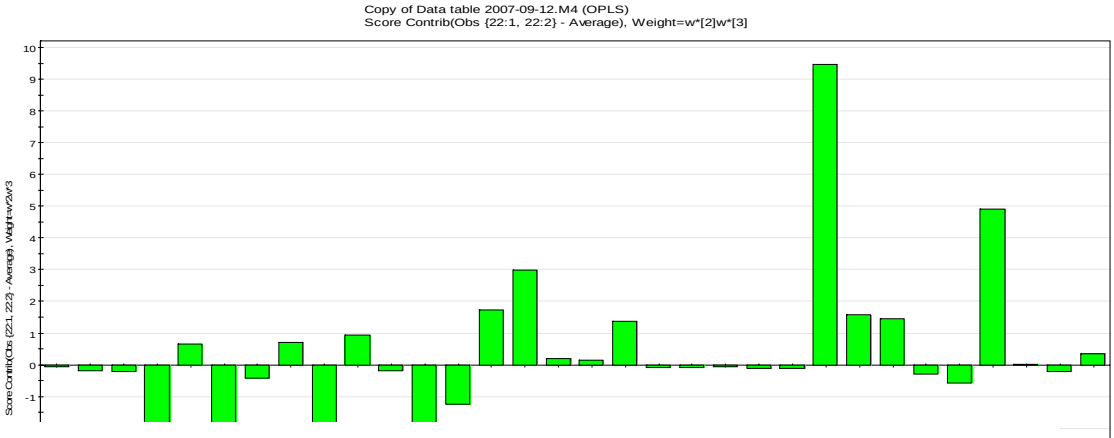

Figure 40. Score contribution plot: Run 22 – decreased O_2 level in the flue gas.

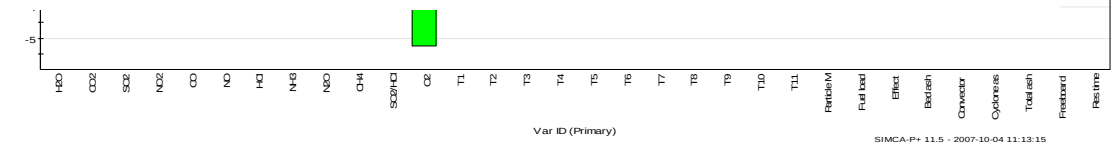

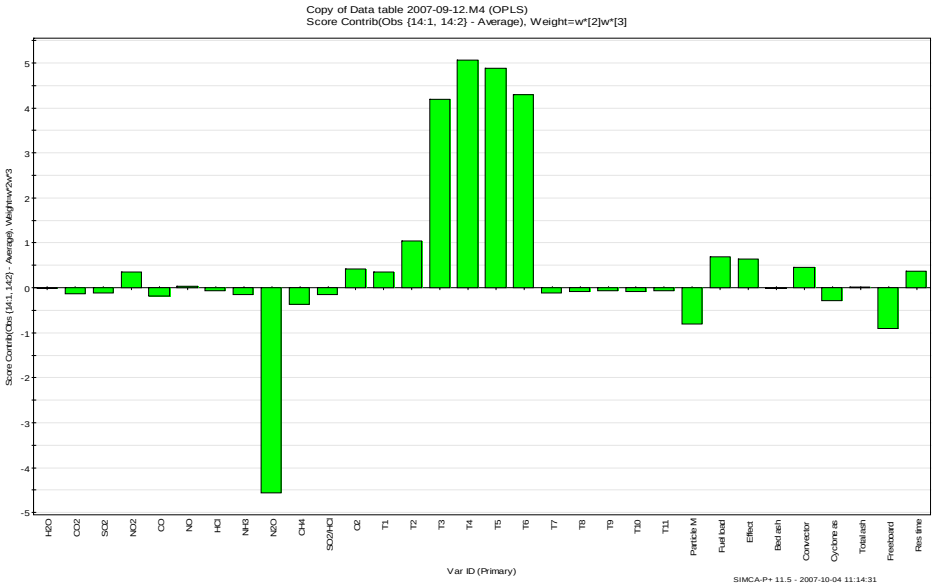

Figure 41. Score contribution plot: Run 14 - increased temperature in the freeboard (950 °C).

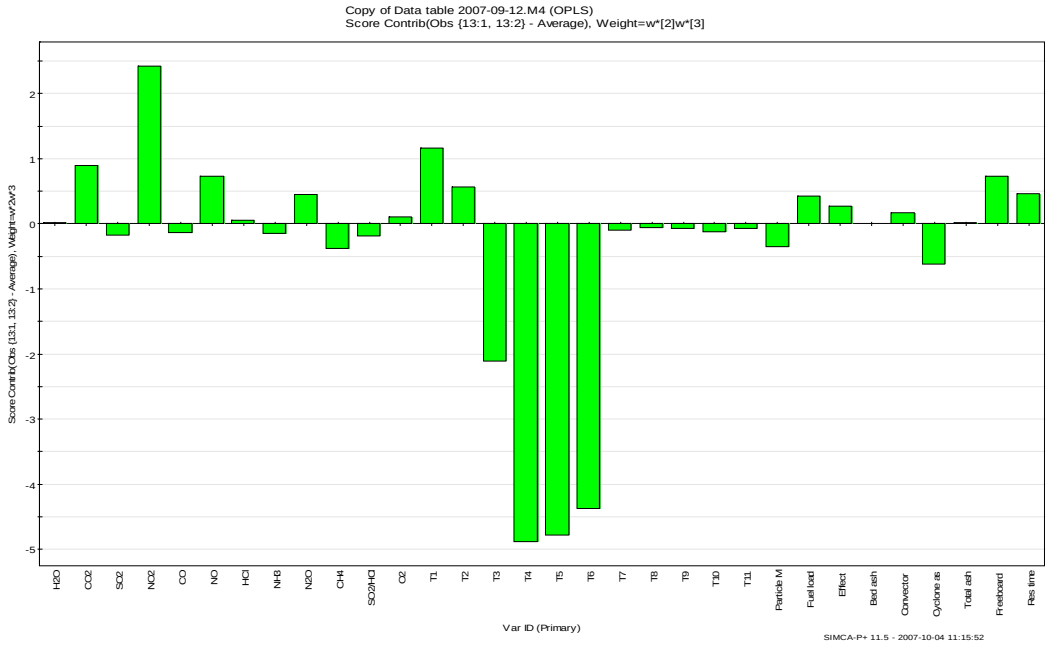

Figure 42. Score contribution plot: Run 13 – Reduced temperature in the freeboard (660 °C).